PACIFIC EARTHQUAKE ENGINEERING
RESEARCH CENTER

Predicting Earthquake Damage in Older Reinforced Concrete Beam-Column Joints

Catherine Pagni
University of Washington

and

Laura Lowes
University of Washington

PEER 2003/17
OCT. 2004

Predicting Earthquake Damage in Older Reinforced Concrete Beam-Column Joints

Catherine Pagni
University of Washington

Laura Lowes
University of Washington

PEER Report 2003/17
Pacific Earthquake Engineering Research Center
College of Engineering
University of California, Berkeley

October 2004

ABSTRACT

Fragility functions are developed that predict the method of repair required for older reinforced concrete beam-column joints damaged by earthquake loading. The results of previous experimental studies are used to develop empirical relationships between damage states and traditional measures of earthquake demand, such as interstory drift, joint deformation, and number of load cycles. Damage states are proposed and linked deterministically with commonly employed MORs; these damage states are characterized by parameters such as concrete crack width, extent of concrete spalling, and yielding and buckling of reinforcement. Probability distributions are fit to the empirical data and evaluated using standard statistical methods. The results of this effort are families of fragility curves that can be used to predict the required method of repair for a damaged joint, as well as a framework for using future experimental data to advance damage assessment of joints.

ACKNOWLEDGMENTS

This work was supported primarily by the Earthquake Engineering Research Centers Program of the National Science Foundation under award number EEC-9701568 through the Pacific Earthquake Engineering Research Center (PEER). Any opinions, findings, and conclusions or recommendations expressed in this material are those of the author(s) and do not necessarily reflect those of the National Science Foundation.

CONTENTS

LIST OF FIGURES

LIST OF TABLES

1 Introduction

1.1 BACKGROUND AND RESEARCH IMPETUS

Performance-based earthquake engineering (PBEE) is the design of a structure to achieve a specific level of performance under a specific level of earthquake loading. Uncertainty, both in prediction of earthquake loading and in prediction of performance, is inherent in the PBEE process. Thus, PBEE includes also the quantification of uncertainty associated with achieving the specified performance objectives. For an earthquake engineer, *performance* has been defined traditionally in terms of structural response parameters, such as interstory drift or inelastic deformation. However, for a building owner, *performance* is defined most clearly in terms of economic impact: the cost of repairing the building and replacing damaged building contents, and the impact this repair and replacement work has on the functionality of the structure. Since an owner must decide what are the appropriate performance objectives for a new or retrofit design, accomplishing PBEE requires prediction not only of structural response under earthquake loading but also of the potential cost and functional impact of earthquake-induced damage.

Figure 1.1 shows the data flow for predicting the economic impact of earthquake-induced damage to a structure. The terms used in Figure 1.1 are part of the nomenclature developed by the Pacific Earthquake Engineering Research (PEER) Center. In this figure the intensity of the earthquake demand is defined by an intensity measure (IM). The structural response parameters traditionally employed by earthquake engineers to characterize performance are identified as engineering demand parameters (EDPs). These parameters are used commonly by engineers today and may be predicted using existing numerical modeling techniques. Empirically derived probabilistic models are required to link EDPs to damage measures (DMs) that characterize the damage state of the building, including structural and nonstructural components. The results of previous research and practical experience provide a basis for associating particular methods of repair (MORs) with specific sets of DMs. There is uncertainty inherent in this process; thus, probabilistic models are appropriate for use in linking DMs with MORs. Finally, standard estimating practice provides a basis for predicting the economic impact of employing a specific repair or replacement method. The cost and impact on building functionality of performing the repair or replacement are identified as "decision variables" (DVs).

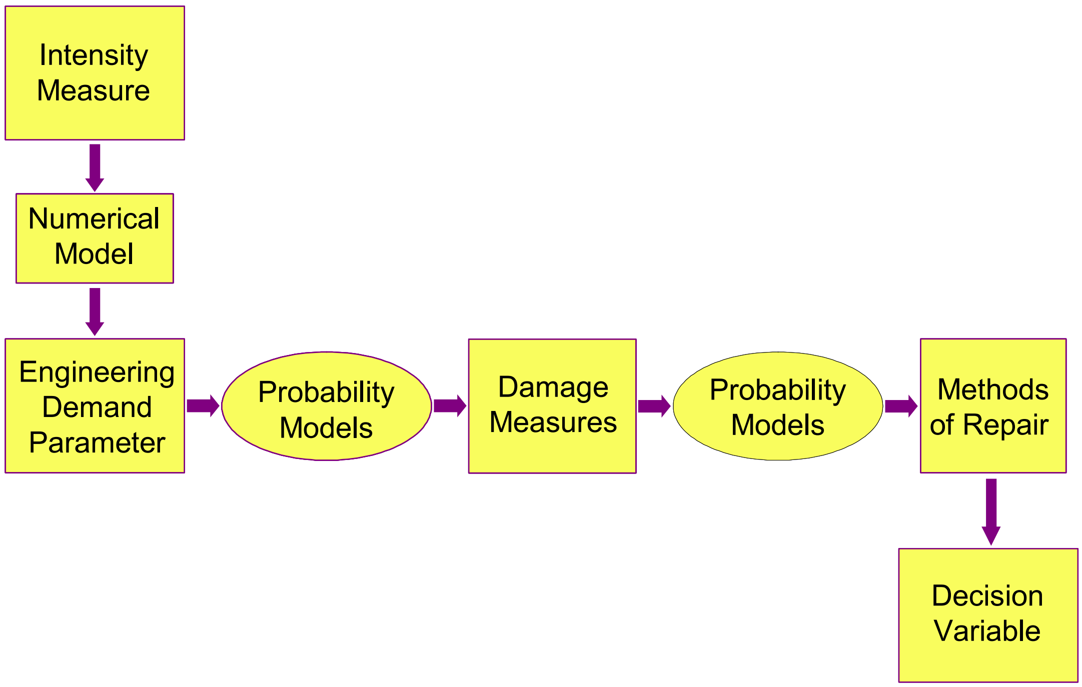

Figure 1.1 Data flow for predicting the economic impact of earthquake damage

The prediction process outlined in Figure 1.1 may be accomplished at multiple levels of sophistication and resolution. One could envision using global structural EDPs, such as roof drift and peak acceleration, to predict the global damage classification for the building, such as *operational*, *repairable*, *life-safe*, or *collapse*. Additional models could then be used to estimate the global repair cost and downtime given the global damage state. One could also envision a much higher resolution assessment of damage, repair and economic impact. For example, using the results of a nonlinear dynamic analysis, models could be used to predict the likelihood of individual structural and nonstructural components exceeding specific damage states. Given the damage state of a component, a specific repair technique can be identified, and the total economic impact of the earthquake is computed as the sum of the repair cost and time for individual components.

The objective of the research presented here is the development of data and models to support the high-resolution, component-specific approach to predicting economic impact. Specifically, data and models are developed to enable engineers to predict the MORs that are required to restore to original conditions older reinforced concrete beam-column joints damaged under earthquake loading. While the data and models developed here are appropriate only for joints, the prediction process as well as the approach used to develop the data and model, is appropriate for any structural component. In applying the process outlined in Figure 1.1 to prediction of the economic impact of beam-column joint damage, the primary components of the process are defined as follows:

- An engineering demand parameter (EDP) is the measure of earthquake demand on a structural component. Here it is assumed that joint EDPs will be estimated using nonlinear dynamic analysis. Since the EDP defines the demand, the EDP must incorporate the characteristics of the component load and deformation history that determine the damage sustained by the joint. Parameters evaluated for use in defining earthquake demands on building joints include interstory drift, number of displacement cycles and total joint shear deformation.
- A damage measure (DM) characterizes the damage sustained by a structural component. In this study, quantitative damage measures are employed such as the maximum concrete crack width, the extent of concrete cracking, and the extent of concrete crushing. Experimental data are used to develop a series of damage states (DS) that describe, using these DMs, the progression of damage sustained by a beam-column joint.
- A method of repair (MOR) comprises a series of tasks that must be accomplished to restore a damaged component to original condition. The results of previous research as well as field experiences are used to identify a series of MOR that are appropriate for use on beam-column joints. These MOR are explicitly linked with groups of damage states.
- Probability models link EDPs to DMs and, ultimately, to MORs. The probability of a component exceeding a specific DS and thus requiring a specific MOR to restore it to original condition is modeled using fragility curves. Specifically, fragility curves define the probability a specific MOR will be required given a specific value of an EDP. Experimental observations of damage in laboratory test specimens are used to develop fragility curves linking EDPs and DMs. Then, the DSs requiring a specific MOR are grouped, and the grouping is used to extend the fragility curves to define the probability that a joint will require a specific MOR given a specific value of the joint EDP.

1.2 RESEARCH OBJECTIVES

The objective of the current study is to collect the data and develop the models required to enable engineers to predict the economic impact of damage in older reinforced concrete beam-column joints. As suggested by the discussion in the preceding section, this includes developing the following data sets and models:

1. Identification of EDPs that define the earthquake demand on joints.
2. Identification of DMs and DSs that characterize the progression of damage in older beam-column joints.
3. Identification of MOR that may be used to restore damaged joints to original conditions.
4. Develop of experimental datasets that link EDPs, DSs, and MORs.
5. Development of fragility curves that enable prediction of the probability that a joint will require a specific MOR given a specific level of an EDP.

1.3 REPORT ORGANIZATION

This report presents the process used to compile data and develop models that enable the prediction of the economic impact of joint damage. Also presented is the application of these tools to predict the impact of joint damage for a case study building subjected to multiple levels of earthquake loading. This information is organized as follows:

Chapter 2 discusses the sources used to complete the project. These sources include research reports, journal papers, manuals of standard practice, texts and interviews. The results of multiple previous experimental investigations of the seismic behavior and design of beam-column joints were used throughout this project to identify EDPs, DMs, and DSs. These experimental investigations as well as the observed behavior and design details for the specific joint specimens are described in Chapter 2. Additionally, the literature pertaining to characterization of damage and repair of reinforced concrete components is reviewed. Finally, literature pertaining to the use of classical statistical methods to generate fragility curves is discussed.

Chapter 3 focuses on the definition of DSs for beam-column joints. While the evaluation of the economic impact of earthquake damage progresses from prediction of EDPs to DMs to DVs, it was found that to generate the required models it was appropriate to first identify DSs characterizing the progression of damage and then link these DSs back to EDPs and forward to

MORs. Data from the previous studies introduced in Chapter 2 are used to quantize the progression of damage into 13 DSs. DMs used to define DSs include maximum crack width, the extent of concrete cracking, and the extent of concrete crushing, as well as binary DSs such as buckling of rebar.

Chapter 4 focuses on identification of the EDPs used to characterize the earthquake demand on the joint. The results of previous experimental investigation are used as a basis for identifying EDPs that are efficient indicators of damage. EDPs considered in the study include direct measures such as interstory drift, number of cycles, and joint strain, as well as numerical indices that are functions of these direct measures.

Chapter 5 identifies and describes MORs that are appropriate for use with older reinforced concrete building joints. These MOR are techniques recommended by current concrete repair manuals and used currently in practice. These MORs are linked explicitly with specific DSs.

Chapter 6 presents the development of models defining the probability of requiring a specific MOR given a specific EDP. The basis of these models is a series of probabilistic models relating EDPs and individual DSs and the pairings between DSs and MORs. Several approaches may be used to generate the probabilistic models using the EDP-DS relationships and the DS-MOR relationships. These different approaches are discussed and evaluated. Standard goodness-of-fit tests determine the best fitting probability distribution.

Chapter 7 summarizes the research results and primary conclusions of the study. Also discussed are future research needs to increase the reliability and facilitate the process of predicting the economic impact of earthquake damage.

2 Literature Review

2.1 INTRODUCTION

The results of previous research and field experience provide a basis for developing models to predict damage and required repair methods for joints. Previous research relevant to the current study is presented in this chapter.

Section 2.2 reviews previous research to develop performance-based earthquake engineering methods and thereby identifies specifically how the results of the current study will contribute to the advancement of performance-based earthquake engineering.

The results of previous experimental investigation, post-earthquake reconnaissance and field experience are used to define (1) DSs that characterize the progression of earthquake damage in joints, (2) the EDPs that can be used to predict the development of these DSs, and (3) the MOR that are appropriate for restoring damaged joints to pre-earthquake conditions. Section 2.3 presents previous experimental investigations from which data are collected to characterize DSs and identify EDPs that efficiently predict damage. Section 2.4 presents post-earthquake reconnaissance reports used to link DSs and MORs.

Epistemic and aleatory uncertainty are inherent to the process of predicting earthquake damage. Thus, probability distributions are used to predict, as a function of an EDP, the MOR required to restore a damaged joint to pre-earthquake conditions. Section 2.5 discusses probability theory, the standard probabilistic models considered in this study, and the "goodness-of-fit" tests used to evaluate the probabilistic models.

2.2 PERFORMANCE-BASED EARTHQUAKE ENGINEERING

Research at the PEER Center and elsewhere to advance PBEE has resulted in an awareness by the earthquake engineering community of the needs (1) to define performance using terms that are understood by and of value to building owners and (2) to employ a probabilistic framework that supports the modeling of uncertainty throughout the process. The PEER framework equation (http://peer.berkeley.edu):

$$\nu(DV) = \iiint G\langle DV|DM\rangle dG\langle DM|EDP\rangle dG\langle EDP|IM\rangle d\lambda(IM) \tag{2.1}$$

was developed to accommodate these needs. In this equation, probabilistic functions link earthquake intensity measures (IMs) with engineering demand parameters (EDPs). This relationship brings the engineer to what was traditionally the end of the analysis. However, the PEER framework equation also provides a basis for going beyond EDPs by employing probabilistic relationships that link EDPs with DMs and subsequently DMs with DVs. Specifically, in Equation 2.1, $\nu(DV)$ is the mean annual probability that the decision variable DV exceeds a specific value, $G\langle DV|DM\rangle$ is the conditional probability that DV exceeds a specific value given a particular value of DM, $dG\langle DM|EDP\rangle$ is the derivative (with respect to DM) of the conditional probability that DM exceeds a limit value given a specific value of EDP, $dG\langle EDP|IM\rangle$ is the derivative (with respect to EDP) of the conditional probability that EDP exceeds a limit value given a specific value of IM, and $d\lambda(IM)$ is the derivative of the seismic hazard curve, $\lambda(IM)$.

The objective of the research presented here is to use the results of previous research to develop the probabilistic relationships linking EDPs with MOR from which DVs may be computed, for one structural component, beam-column building joints. The PEER framework equation provides a basis for employing these models in combination with other similar component-specific models to assess the economic impact of earthquake damage.

2.3 EXPERIMENTAL DATA

The initial phase of the research effort identified experimental data characterizing the progression of earthquake damage in older beam-column joints. The criteria used to choose laboratory test specimens, the characteristics of the experimental test specimens, and variation in test specimens that could be expected to affect the observed damage patterns and progression are discussed in the following sections.

2.3.1 Criteria Used to Identify Appropriate Laboratory Test Specimens

Three criteria were used to identify experimental data sets for use in this study. First, only laboratory specimens with design details representative of pre-1967 construction were included in the study. Seismic design provisions were introduced into the UBC in 1967 and the ACI code in 1971. Prior to this, design recommendations did not explicitly address joint design. Mosier (2000) reviewed 15 buildings designed prior to 1979 for construction on the West Coast to identify typical design parameters for this period. Mosier concluded that most buildings designed before 1967, and many building designed between 1967 and 1979, had detailing that could be expected to result in nonductile response under earthquake loading. Table 2.1 lists Mosier's findings for design parameters that could be expected to determine the earthquake performance of beam-column joints. Only joint test specimens with design parameters that fell within the ranges observed by Mosier (2000) for pre-1967 design were used in the current study, with two exceptions:

- 5 of the 21 specimens included in this study were constructed with transverse joint reinforcement. For these 5 specimens, volumetric transverse steel ratios ranged from 0.2% to 0.4%. These volumes were considered to be sufficiently low, in comparison with the post-1967 average of 0.9%, to be representative of pre-1967, rather than post-1967 construction.
- 3 of 21 specimens included in this study had beam bottom reinforcement that was discontinuous through the joint. For these specimens, the bond index was higher than the maximum observed by Mosier (2000) for pre-1967 construction.

Table 2.1 Design details for pre-1979 beam-column joints

	Volumetric Transverse Steel Ratio (%)			Shear Stress Demand / f'c			Beam Bar Bond Index, $\mu = \frac{d_b f_y}{2 l_d \sqrt{f_c}}$		
Design year	ave.	min.	max.	ave.	min.	max.	ave.	min.	Max.
Pre-1967	0.0	0.0	0.2	0.21	0.09	0.30	21	12	38
1967-1979	0.9	0.0	2.1	0.15	0.06	0.29	23	14	43

Note: In defining the bond index, μ, d_b is the diameter of the reinforcing bar, f_y is the yield strength of the reinforcing steel, l_d is the anchorage length within the joint assumed to be equal to the column depth and f_c is the concrete compressive strength and units are inches and pounds.

Second, only laboratory test specimens with the same basic configuration and load pattern were used. All of the specimens considered in the study were subassemblages from two-dimensional building frames and comprised the joint, the beams framing into the joint and extending to mid-span, and the columns framing into the joint and extending to mid-height. Lateral loading was applied as a shear force at the top of the column and reacted by shear forces at the base of the column and beam ends. If it is assumed that beams and columns develop a point of contra-flexure at mid-span under earthquake loading, then this laboratory load distribution is representative of earthquake loading in a real structure. Simulated earthquake load was applied pseudo-statically by forcing the top of the column through a prescribed cyclic displacement history (relative to the beam ends and column base) consisting of one or more cycles to increasing maximum displacement demands. In some cases, a constant axial load was applied at the top of the column to simulate gravity load.

Third, a specimen was included in this study only if sufficient data characterizing the progression of damage in the beam-column joint were provided by the researchers. While all experimental researchers provide data characterizing the load-displacement response of laboratory test specimens, the detail and consistency with which damage data are reported varies substantially. In many cases, the lack of sufficient damage data eliminated joint specimens from use in this study.

2.3.2 Experimental Data Used in the Study

A review of the literature resulted in five test programs and 21 test specimens that met the above criteria:

- *Meinheit and Jirsa (1977)* investigated the impact of joint transverse reinforcement on response. Data from one (MII) of the 11 specimens tested by Meinheit and Jirsa were used. Sufficient data characterizing the progression of damage are provided only for this specimen.
- *Pessiki et al. (1990a)* investigated the earthquake response of older building components, including joints. Pessiki et al. conclude that the joint failure mechanism depends on the amount of reinforcing steel within the joint and beam-bar anchorage lengths. Data from seven (P2-P5, P7-P9) of the Pessiki test specimens were used.

- *Joh et al. (1991a, 1991b)* investigated the impact on earthquake response of (1) joint transverse reinforcement, (2) beam transverse reinforcement, and (3) torsion due to beam eccentricity. They conclude that increasing the volume of transverse reinforcement results in decreased bar slip, increased energy dissipation, and increased post-cracking joint stiffness. Only specimens with concentric beam-column connections and low transverse steel volumes were used in the current study. This included three specimens from the Joh et al. investigations (JXO-B8-LH, JXO-B1, and JXO-B2).
- *Walker (2001) and Alire (2002*) evaluated the impact of joint shear stress and load history on performance. These studies conclude that joints maintain strength and adequate stiffness when drift demand is less than 1.5% and shear stress demand is less than $10\sqrt{f'_c}$. Data from ten of the specimens in these two test series were used (PEER *, CD *, PADH *).

Design details and loading data for these specimens are listed in Table 2.2.

Table 2.2 Design details and load data for experimental test specimens

Specimen	f'c (psi)	Shear Stress Demand / f'c	Shear Stress Demand / sqrt(f'c) (psi)	Transverse Steel Volume Ratio (%)	Maximum Bond Index, μ	Column Axial Load / f'cAg	Drift History*	Column Splice Above Joint	Ratio of Beam to Column Width
PEER14	4606	0.16	10.9	0.00	18.7	0.11	Standard	no	1.00
PEER22	5570	0.20	14.6	0.00	24.9	0.09	Standard	no	1.00
CD1514	4322	0.18	11.6	0.00	19.3	0.12	High-cyc.	no	1.00
CD3014	6171	0.14	11.3	0.00	16.1	0.08	High-cyc.	no	1.00
CD3022	5533	0.21	15.5	0.00	25.0	0.09	High-cyc.	no	1.00
PADH14	6218	0.15	11.7	0.00	16.1	0.08	Unsym.	no	1.00
PADH22	5259	0.22	15.7	0.00	25.6	0.10	Unsym.	no	1.00
PEER09	9500	0.13	12.6	0.00	16.7	0.10	Standard	no	1.00
PEER15	9500	0.19	18.7	0.00	26.7	0.10	Standard	no	1.00
PEER41	5000	0.17	12.2	0.00	29.6	0.10	Standard	no	1.00
P2	5000	0.19	13.2	0.00	34.8	0.27	Standard	yes	0.88
P3	4000	0.21	13.2	0.00	34.6	0.34	Standard	yes	0.88
P4	4000	0.20	12.7	0.00	34.6	0.34	Standard	yes	0.88
P5	4000	0.22	13.6	0.23	38.0	0.34	Standard	yes	0.88
P7	3000	0.19	10.5	0.00	52.5	0.46	Standard	yes	0.88
P8	3000	0.19	10.3	0.00	39.4	0.46	Standard	yes	0.88
P9	4000	0.15	9.60	0.00	39.5	0.10	Standard	yes	0.88
MII	6060	0.25	19.7	0.44	25.1	0.25	Standard	no	0.85
JXO-B1	3901	0.12	7.51	0.27	19.9	0.17	Standard	no	0.67
JXO-B2	3269	0.24	13.8	0.27	19.9	0.17	Standard	no	0.50
JXO-B8	3429	0.19	11.1	0.27	19.5	0.15	Standard	no	0.93
Min.	3000	0.12	7.5	0.00	16.1	0.08			0.50
Max.	9500	0.25	19.7	0.44	52.5	0.46			1.00
C.O.V.	0.36	0.19	0.22	1.90	0.36	0.67			0.14

Note: A *standard* drift history comprises 1 to 3 cycles to increasing maximum drift demands, a *high-cycle* history comprises 10 or more cycles to increasing maximum drift demands, and an *unsymmetrical* history comprises multiple cycles to varying maximum and minimum drift demands.

2.3.3 Factors That Determine the Earthquake Response of Joints

The specimens listed in Table 2.2 have design details representative of pre-1967 construction and were subjected to similar simulated earthquake load patterns in the laboratory. However, there are differences in design and load parameters that could be expected to result in some variability in damage patterns and progression under earthquake loading. These differences include the following:

- *Nominal Joint Shear Stress Demand:* The results of multiple studies indicate that joint performance, as defined by the extent of damage and/or the drift level at which strength loss initiates, deteriorates with joint shear stress demand (Walker 2001; Hakuto et al. 1997; Durrani and Wight 1982; Meinheit and Jirsa 1981).

- *Transverse Steel Ratio:* The results of multiple studies suggest that increasing the volume of joint transverse reinforcement reduces joint damage and delays failure (Joh et al. 1991a; Pessiki et al. 1990b; Durrani and Wight 1982; Hanson and Conner 1967).
- *Bond Index:* For joints with continuous beam reinforcement, the bond index is the average bond stress demand along the beam reinforcing steel, assuming that the steel yields in compression and tension on opposite sides of the joint. The results of multiple studies indicate that increased bond stress demand results in increased damage and reduced drift capacity (Alire 2002; Leon 1990; Park and Ruitong 1988).
- *Discontinuous Beam Reinforcement:* Three of the joint specimens (P7, P8, and P9) have beam longitudinal reinforcement that is not continuous through the joint. Discontinuous beam reinforcing results in particularly short anchorage lengths, which in turn could be expected to result in increased joint damage and limited drift capacity under earthquake loading.
- *Column Axial Load:* For many of the laboratory test specimens used in this study, axial load was applied at the top of the column and maintained at a constant level throughout the test. Bonnaci and Pantazopoulou (1993) assembled data from 86 joint tests and conclude that column axial load has no discernible affect on joint *strength*. Mosier (2000) reaches a similar conclusion using a database of 29 test programs and considering data only from joints that failed in shear. However, the impact of column axial load on joint *performance* is not well documented in the literature. Bonnaci and Pantazopoulou (1993) hypothesize that axial load affects joint deformation but note that insufficient data are available to test this hypothesis. Kitiyama et al. (2000) conclude, on the basis of data from numerous joint tests conducted in Japan, that higher axial load results in more rapid deterioration of the joint load-transfer mechanism. Given the limited impact of column axial load on joint strength and the limited data characterizing the impact of axial load on joint performance, it is unclear how significant an impact the 67% variation in column axial load (Table 2.2) has on the observed damage patterns.
- *Column Splice:* Seven of the joint specimens have column longitudinal steel that is spliced above the joint. For these joints, splice lengths and confining reinforcement are

considered inadequate by today's standards. These inadequately designed splices may affect joint strength and drift capacity as well as the progression of joint damage under simulated earthquake loading.

2.4 METHODS OF REPAIR

Federal Emergency Management Agency (FEMA) and American Concrete Institute (ACI) documents providing guidelines on repair, the results of previous experimental studies, and interviews with industry professionals were used as a basis for identifying appropriate repair methods for joints. These MOR for joints presented in Chapter Five were determined using the information provided in the following sources.

Government documents and design codes provide concise instruction for the identification and repair of damaged reinforced concrete. A series of documents regarding repair to earthquake damaged were prepared by the Applied Technology Council (ATC) and funded by FEMA in the late 1990s. Within the series, repair techniques appropriate for various types of buildings are listed. For example, Chapter 4 of *FEMA 308: Repair of Earthquake Damaged Concrete and Masonry Buildings*, contains a list of repair techniques similar to those presented in this report. The repair techniques are categorized as *Cosmetic Repair*, *Structural Repair*, *and Structural Enhancement*. The materials, equipment, and method of execution are provided as well as the limitations for the extent of damage to be repaired.

Several ACI publications discuss repair of concrete structures. *ACI Special Publication 21* (1968) discusses the application and effectiveness of repair using epoxy resin. *The Concrete Repair Guide, ACI 546R-96* (1996) addresses multiple repair methods, and one section of this document is devoted to beam-column joints.

Multiple research studies have addressed the repair of reinforced concrete components damaged as a result of earthquake loading. Experimental investigations that included testing, repair, and retesting of beam-column joints were conducted by Karayannis (1998), Filiatrault (1996), Tasai (1992), and French et al. (1990). The results of these studies are of particular interest to the current investigation, as they help to validate specific repair methods. Filiatrault (1996), Tasai (1992) and French et al. (1990) all provide data characterizing the response of joints repaired using epoxy resin. Karayannis (1998) evaluates the effectiveness of cementitious material used for patching spalled and crushed concrete.

Other studies document repair strategies employed in the field following seismic events. Jara et al. (1989) document repair done following the 1985 Mexico City earthquake. This study suggests that the repair techniques employed restored concrete components to the original strength and serviceability.

Using the information provided in these references, a list of MORs was assembled for the current study. The list was presented for feedback and refinement to practicing engineers and contractors with experience in specifying and conducting repair of damaged reinforced concrete buildings and bridges. Consultants included Steve Savage, a structural engineer from Coughlin, Porter, and Lundeen of Seattle; Harvey Coffman and Jugesh Kapure, engineers from the Washington State Department of Transportation; Jared Cole a project engineer at T.Y. Lin in San Diego; Dave Juraszek of Juraszek Concrete Construction, and Roger Runacres of Contech Services, Inc. The interview transcripts highlighting relevant information discussed during the in-person interviews are provided in the appendix.

2.5 PREDICTING DAMAGE AS A FUNCTION OF DEMAND

Fragility functions define the probability of a joint requiring a specific MOR given a measure of earthquake demand as defined by an EDP. To facilitate prediction of the required MOR, fragility functions are standard probability distributions. For the current study, three standard probability distributions were considered to model the data and thereby create fragility functions. Three goodness-of-fit tests were used to evaluate these distributions. These topics and the references used to develop fragility functions are discussed in following sections.

2.5.1 Fragility Functions

Fragility functions define the probability of reaching or exceeding a level of damage given a specific level of earthquake demand. Examples of fragility functions in the literature include Saxena et al. (2000), who develop fragility functions for multi-span concrete highway bridges with earthquake demand defined by peak ground acceleration and Porter (2002) who develops fragility functions for a number of structural and nonstructural building components with earthquake demand defined by a component-specific parameter. Shinozuka et al. (2000) provides recommendations for developing fragility functions using empirical data.

2.5.2 Testing Goodness of Fit

Shinosuka et al. (2000) recommend the use of hypothesis testing to evaluate the goodness of fit of standard probability functions for definition of fragility functions. In the current study, three standard goodness-of-fit tests, the chi-square (χ^2) test, the Kolmogorov-Smirnov (K-S) and the Lilliefors test were used to identify a preferred standard CDF for use in modeling empirical data.

The χ^2 test compares the empirical and theoretical probability density function (PDF), which is the derivative of the CDF with respect to the random variable. The observed data are subdivided into m intervals and the number of observations within each interval, n_i, is compared with the theoretical number of observations, e_i. It can be shown (Hoel 1962) that the quantity

$$\sum_{i=1}^{m} \frac{(n_i - e_i)^2}{e_i} \tag{2.2}$$

approaches the χ^2 distribution with $f = m$-1-k degrees of freedom as n approaches ∞. Here m is the number of intervals and k is the number of parameters in the theoretical distribution. The theoretical distribution is acceptable, at the significance level α, if

$$\sum_{i=1}^{m} \frac{(n_i - e_i)^2}{e_i} < c_{1-\alpha,f} \tag{2.3}$$

where $c_{1-\alpha,f}$ is the value of the χ^2 distribution with f degrees of freedom at a CDF value of (1-α). For the current study, m was chosen as 5 and α was chosen to be 5%, with the result that $c_{1-\alpha,f} = 5.992$ for all cases. For the current study, the MATLAB (2002) function **icdf** was used to compute $c_{1-\alpha,f}$.

In applying the χ^2 test, it is important to note that the quality of the test is reduced by a small sample size. Specifically, it is recommended that m, the number of intervals, and e_i, the number of observations in each interval, be at least 5 for satisfactory results (Haldar and Mahadevan 2000) and that the total number of data points exceed 50 (Kottegoda and Rosso 1997). In the current application, the requirements for satisfactory performance of the χ^2 test on the number of intervals is met for all of the data; however neither the requirements on the number of observations per interval nor the requirement on the total number of data points is met for any of the EDPs. Thus, the results of the χ^2 are questionable.

The K-S test compares the empirical and theoretical CDFs. In general, the K-S test has two advantages over the χ^2 test: (1) it is appropriate for use for any size sample and (2) it is more powerful that the χ^2 test (Lilliefors 1967). However, the K-S test is appropriate only for testing distributions with known parameters (Kottegoda and Rosso 1997; Lilliefors 1967). This is not the case in the current study, since distribution parameters are computed using the data. Lilliefors (1967) shows that in this case, the K-S test is extremely conservative for rejection of a distribution, making it extremely unconservative for acceptance of a distribution. Thus, for the current application, in cases where the probability of acceptance of the distribution is low, the validity of this acceptance is questionable.

The K-S test requires computation of D_n, the maximum difference between the two CDFs:

$$D_n = \max\left|F_X(x_i) - S_X(x_i)\right| \tag{2.4}$$

where $F_X(x_i)$ is the theoretical CDF computed for the ith observation and $S_X(x_i)$ is the empirical CDF for the ith observation (note that the value of the value of the $S_X(x_i)$ computed at the ith observation is equal to the percentage of observations less than or equal to the ith observation). D_n is a random variable with a distribution that depends on the sample size n and the CDF of D_n is related to the significance level α as

$$P(D_n \leq D_n^\alpha) = 1 - \alpha \tag{2.5}$$

According to the K-S test, if D_n is less than or equal to the tabulated value of D_n^α, then the theoretical distribution is acceptable at the significance level α. The MATLAB function **ktest** is used to accomplish the K-S test with a chosen significance level of 5%.

David and Johnson (1948) note that the K-S test can be modified to account for computation of distribution parameters using sample data. Lilliefors (1967) does this for the case of the normal distribution, thereby developing what is commonly known as the "Lilliefors" test. This test is appropriate for the small sample sizes and is exact. The Lilliefors test is identical to the K-S test with the exception that the tabulated test values, D_n^α, are computed on the basis that the sample data are used to compute the mean and standard deviation of the distribution. For the current study, this test can be used to evaluate the acceptability of the lognormal distribution. The MATLAB function **lillietest** is used to accomplish the Lilliefors test with a significance level of 5%.

2.5.3 Distribution Selection

Three standard probability functions were considered for use in modeling the damage data and evaluated using the statistical goodness-of-fit tests described above:

- Lognormal distribution: Commonly employed distribution that includes only positively valued data.
- Weibull distribution: Less commonly used distribution. The distribution allows for a stronger influence of extreme-valued data. This is desirable for the current application where small-demand values are important.
- Beta distribution: Less commonly used distribution. This distribution allows for an upper and lower bound to be defined for the distribution, which is desirable for the current application. Note that for this application the lower bound for all CDFs was defined to be 0.0 and the upper bound was defined by the maximum of the data.

Additionally, the empirical distribution, often referred to as the "stepwise distribution," was used in evaluating the goodness of fit of the analytical distributions.

A probability distribution may be defined in two ways. The first is as a probability density function (PDF). This function, specified in the following sections as $f_x(x)$, defines the probability of an observation having the value *x*. The second way in which a probability distribution may be defined is as a cumulative distribution function (CDF). This function, specified typically as $F_x(x)$ or, for the stepwise distribution $S_x(x)$, defines the probability that an observation will meet or exceed a value *x*. The PDF and CDF are related in that the PDF is the derivative of the CDF with respect to the random variable *x*. The fragility functions that are developed as part of this study are cumulative distribution functions (CDFs) with EDP taken as the random variable *x*.

2.5.3.1 Lognormal distribution

The PDF for the lognormal distribution is expressed as

$$f_x(x) = \frac{1}{\sqrt{2\pi}\zeta_x x}\exp\left[-\frac{1}{2}\left(\frac{\ln x - \lambda_x}{\zeta_x}\right)^2\right] \quad 0 \le x < \infty \tag{2.6}$$

where x is the random variable, this case EDP, and the lognormal parameters, λ_x and $\zeta_x^{\ 2}$, are related to the mean and the variation of x as follows:

$$\lambda_x = \ln \mu_x - \tfrac{1}{2}\zeta_x^2 \tag{2.7a}$$

$$\zeta_x^2 = \ln\left[1 + \left(\frac{\sigma_x}{\mu_x}\right)^2\right] = \ln\left(1 + \delta_x^2\right) \tag{2.7b}$$

where μ_x is the mean of the x and σ_x is the standard deviation. Note that the data set must be all positive real numbers. These parameters can also be called the "expected values," or normal parameters, of ln x.

2.5.3.2 Weibull distribution

The Weibull distribution is considered an asymptotic distribution where the smallest values of the data set are limited to the lower bound, ε. To represent the data considered here, the value of ε is set to zero.

$$f_x(x) = \frac{k}{w}\left(\frac{x}{w}\right)^{k-1} \exp\left[-\left(\frac{x}{w}\right)^k\right] \quad x \geq 0 \tag{2.8}$$

where the parameters of the Weibull distribution, k and w, are evaluated using the mean, μ_x, and coefficient of variation, δ_x, of x as follows:

$$k = \delta_x^{-1.08} \tag{2.9a}$$

$$w = \frac{\mu_x}{\Gamma\left(1 + \dfrac{1}{k}\right)} \tag{2.9b}$$

where the Γ is the gamma function. Γ(1+x) may be evaluated using the polynomial approximation when $0 \leq x \leq 1$. Since k is a positive value for the data considered here, the polynomial approximation for the gamma function may be used. The polynomial approximation is a fifth-order equation:

$$\Gamma(1+x) = 1 + a_1 x + a_2 x^2 + a_3 x^3 + a_4 x^4 + a_5 x^5 + \varepsilon(x) \tag{2.10a}$$

$$a_1 = -0.575 \quad a_2 = 0.951 \quad a_3 = -.06999 \quad a_4 = 0.425 \quad a_5 = -0.101 \tag{2.10b}$$

$$|\varepsilon(x)| \leq 5 \times 10^{-5} \tag{2.10c}$$

2.5.3.3 Beta distribution

The beta distribution is defined by the upper- and lower-bound limits, *a* and *b*. Typically, the values of *a* and *b* are determined using the smallest and largest data points included in each set. For the current study, *a* is defined to be zero. Variations of the parameters, *q* and *r*, generate a wide range of PDFs from parabolic to linear to exponential.

$$f_X(x) = \frac{1}{B(q,r)} \frac{(x-a)^{q-1}(b-x)_{r-1}}{(b-a)^{q+r-1}} \quad a \le x \le b \tag{2.11}$$

The beta function, $B(q,r)$, is calculated using the gamma function. The gamma function may be evaluated using the polynomial approximation as described in Equation 2.10, if the criteria for *x* are met.

$$B(q,r) = \frac{\Gamma(q)\Gamma(r)}{\Gamma(q+r)} \tag{2.12}$$

The parameters, q and r, are related to the mean and the coefficient of variation of x as follows:

$$\mu_x = a + \frac{q}{q+r}(b-a) \tag{2.13a}$$

$$\delta_x = \frac{qr}{(q+r)^2(q+r+1)}(b-a)^2 \tag{2.13b}$$

Figure 2.1 shows the impact of the parameters *q* and *r* on the probability density function. The probability of an event is the integration of the area under the curve.

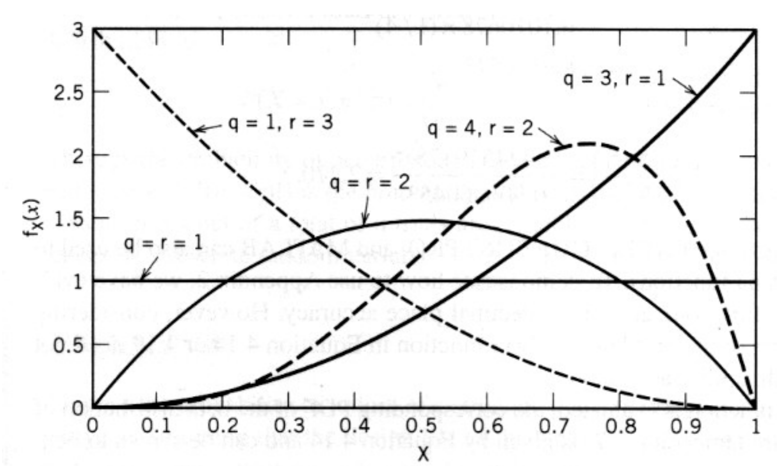

Figure 2.1 Beta probability density function (from Haldar and Mahadevan 2000)

2.5.3.4 Stepwise CDF

A useful comparative cumulative distribution is the stepwise CDF, $S_n(x_i)$. This CDF utilizes the rank of each data point to determine the probability of occurrence. Repeating data values are included in the rank sequence.

$$S_x(x) = \begin{Bmatrix} 0 & x < x_1 \\ \dfrac{m}{n+1} & x_m \leq x \leq x_{m+1} \\ 1 & x \geq x_n \end{Bmatrix} \tag{2.14}$$

where m_i is the rank of each data point, x_i, and n is the total number of data points in the set. The extreme values, x_1 and x_n, are defined by the range of the data set.

2.5.4 Method of Maximum Likelihood

Two different methods may be used to calibrate a probability distribution given an empirical data set: the method of moments and the method of maximum likelihood (Haldar and Mahadevan 2000). Using the method of moments, the probability distribution parameters are computed from the mean and variance of the population, which are estimated using the sample data. Because the sample data provide only estimates of the mean and variance of the population, this method introduces additional uncertainty into the calculation process. To avoid this error, the method of maximum likelihood may be used to determine the distribution parameters. Using this method, a likelihood function is defined:

$$L = \prod_{i=1}^{n} f_X(x_i, p) \tag{2.15}$$

where f_X is the PDF, x_i is an individual data point, and p is the vector of distribution parameters. The distribution parameters are computed to maximize this likelihood function. This approach is used in the current study. The MATLAB function **mle** was used to compute distribution parameters using the method of maximum likelihood.

3 Damage Measures

3.1 INTRODUCTION

Damage measures, DMs, describe the damage sustained by a component during an earthquake. In this study, damage is quantized into discrete damage states (DSs). The results of previous laboratory studies, post-earthquake reconnaissance, and field experience are used as bases for identifying a series of DSs that (1) best characterize the progression of damage in reinforced concrete beam-column joints and (2) best determine what is the appropriate MOR for the component. The identification and characterization of DSs represents the first step in developing models for use in predicting the economic impact of earthquake-induced damage.

The DSs identified in this study are defined by DMs that are visually observable in the laboratory and in the field as well as by damage measured that require the use of laboratory instrumentation. Section 3.2 presents the DSs used in this study. Sections 3.3 through 3.5 provide additional information about DSs that are defined on the basis of external, visually observable damage measures such as concrete cracking, spalling and crushing, and joint failure. Section 3.6 provides additional information about DSs that are defined on the basis of laboratory instrumentation data.

3.2 DAMAGE STATES

The results of previous laboratory studies, post-earthquake reconnaissance and field experience are used as the bases for identifying a series of 12 states that define the progression of damage in reinforced concrete beam-column building joints. DSs are defined on the basis of external, visually observable damage measures such as concrete crack width, the extent of concrete cracking and crushing, and bond degradation as represented by damage to bond-zone concrete or the opening of large flexural cracks at the frame member-joint interface. The majority of the DSs presented in this research are external and visually observable in the laboratory and in the field.

Two DSs are defined on the basis of laboratory instrumentation measurements rather than external, visually observable measurements. These DSs are defined by reduction in the measured strength of the subassemblage strength. These DSs are referred to as "strength-based." Strength-based DSs are particularly valuable in predicting economic loss as a function of EDPs because, while few researchers provide comprehensive data characterizing the progression of visually observable damage, all researchers provide data defining subassemblage strength.

3.2.1 Progression of Damage

The damage measures presented in this paper are the result of analysis of the progression of damage recorded in the experimental reports presented in Section 2.4. The initial order of progression is determined using the most detailed damage reports and compared against the damage reported in the remaining selected specimens. The progression of the damage measures is essential to the relationship between the damage evident through inspection and the damage evident through instrumental read-outs.

3.2.2 Damage States

The DSs sustained by a beam-column joint in order of increasing earthquake demand are

0. Initial cracking at the beam-column interface
1. Initial cracking within the joint area
2. Crack width is less than 0.02 in. (5 mm)
3. Crack width is greater than 0.02 in. (5 mm)
4. Beam longitudinal reinforcement yields
5. Crack width is greater than 0.05 in. (1.3 mm)
6. Spalling of at least 10% joint surface concrete
7. Joint shear strength begins to deteriorate
8. Spalling of more than 30% joint surface concrete
9. Cracks extend into the beam and/or column
10. Spalling of more than 80% joint surface concrete
11. Crushing of concrete extends into joint core
12. (a) Buckling of longitudinal steel reinforcement
12. (b) Loss of beam longitudinal steel anchorage within the joint core
12. (c) Embedded beam longitudinal steel reinforcement pull-out

3.3 CRACKING

The first indication of damage in the joint is cracking of the concrete. Initially, cracking occurs at the perimeter of the joint due to flexural loading of the beams. As loading progresses, diagonal cracks occur within the joint due to shear loading of the joint core. If cracking is severe, repair is required using epoxy resin. Damage States 0, 1, 2, 3, 5, and 9 are all characterized by the width and extent of concrete cracking.

Ideally, in monitoring cracking for use in predicted required repair, one would consider the maximum crack width under zero lateral loading, since this is the damage measure used traditionally in the field to determine the need for repair. However, relatively few researchers provide information about residual crack widths; instead information about maximum crack width at peaks in the displacement history is recorded. In the current study, maximum crack width and the extent of cracking at a displacement peak is used as a conservative estimate of residual crack width. At low load levels, maximum crack width is likely a poor indicator of residual crack width, since narrow cracks typically close under removal of load. However, at moderate to severe load levels, maximum crack width under loading is a more reliable indicator of residual crack width, as wider cracks, which often become filled with debris, are less likely to close under load removal.

3.3.1 Damage State 0

Damage State 0 is defined by flexural cracking at the beam-joint interface. These cracks are the first to appear under lateral loading of a joint subassemblage. In all of the experimental tests reviewed, these cracks form before cracks form within the joint. These cracks are flexural cracks that form at the point of maximum flexural demand in the beam, which is at the beam-joint interface. The cracks typically initiate at the tension face of the beam, which is the joint corner, and propagate vertically as seen in Figure 3.1. The vertical cracks at the beam-joint interface shown in this figure formed at drift levels of 0.25% and 0.5%.

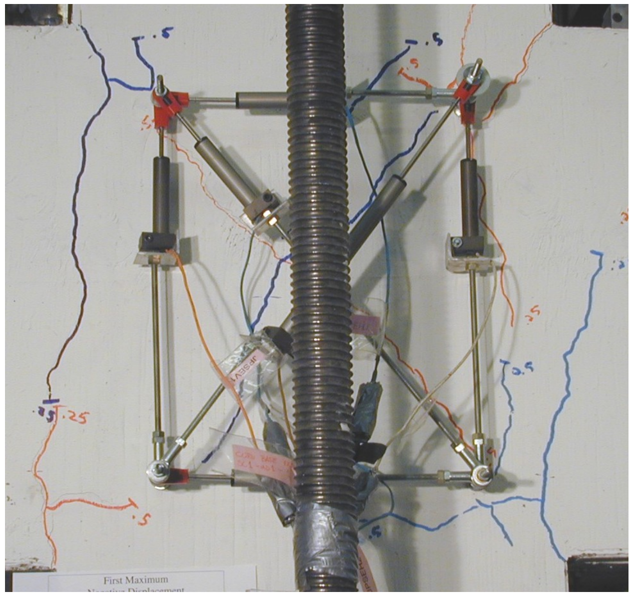

Figure 3.1 Joint Specimen PEER 22 at Damage State 2 (Walker 2001)

3.3.2 Damage State 1

Damage State 1 is defined by initial cracking within the joint. These cracks are of hairline, i.e., immeasurable, width. Structural engineers do not consider repair of these cracks to be necessary (Savage 2003; Coffman and Kapur 2003). Figure 3.1 shows this type of cracking; in this figure cracks in the center of the joint, behind external displacement transducers and loading apparatus, are marked in red and blue.

3.3.3 Damage States 2, 3, and 5

Damage States 2, 3, and 5 defines stages of crack opening. Defining the increments of cracks width appeared to be important initially when investigating the repair of cracked concrete. Cracks in damaged reinforcement concrete buildings after the Mexico City earthquake were repaired based on the width of the cracks (Jara et al. 1989); cracks smaller than 0.02 in. were not repaired. Similarly, ACI 318-95 (1995) defines cracks having a width less than 0.013 in. for exterior and 0.016 in. for interior components as appropriate for no repair. Crack widths greater than 0.016 in. are at risk for corrosion of the reinforcing steel or will not allow transfer of stresses through the aggregate. These sources of repair determined the crack widths defining Damage States 2, 3, and 5. Figure 3.2 shows cracking representative of Damage State 5.

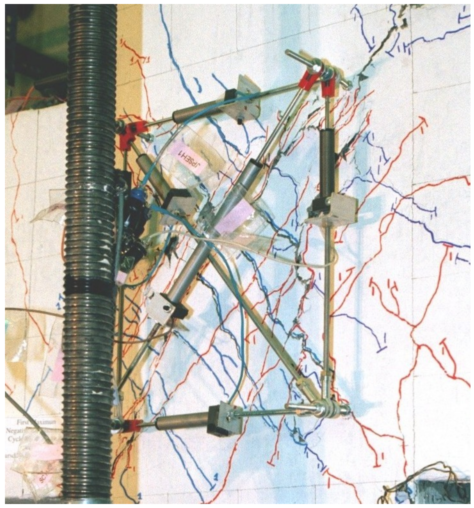

Figure 3.2 Joint Specimen CD30 22 exhibits Damage State 5 (Walker 2001)

3.3.4 Damage State 9

Damage State 9 describes cracking that initiates within the joint and propagates into the adjacent beams or columns. Typically, the crack progresses along the reinforcement and may be considered indicative of a splitting-type bond failure. Figure 3.3 shows an exterior joint subassemblage with cracking representative of Damage State 9; cracking has propagated into the column on both sides of the joint. While this type of cracking is most common in exterior joints, three of the interior joint specimens exhibited this damage prior to failure.

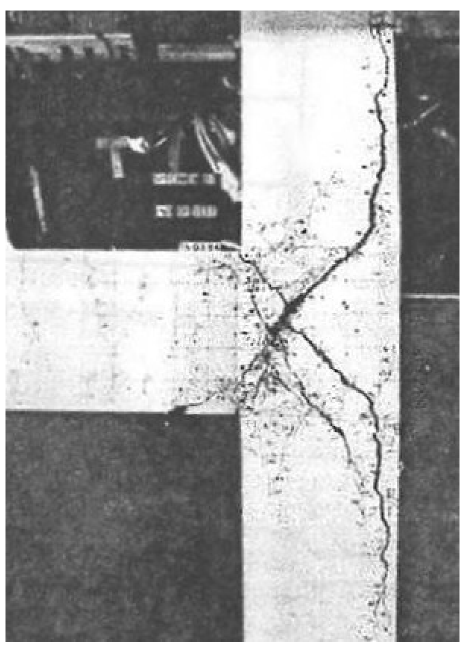

Figure 3.3 Exterior joint specimen exhibits Damage State 9 (Hakuto et al. 2000)

3.4 CONCRETE SPALLING AND CRUSHING

Damage States 6, 8, 10, and 11 are descriptions of damage to the joint concrete. These DSs are defined by the extent of concrete spalling and crushing. Damage States 6, 8, and 10 refer to the extent of concrete spalling. For the current study, concrete spalling is defined as the breaking off of the concrete layer covering the outermost layer of reinforcing steel. For a few of the joints, this outermost layer is transverse steel, but for most of the joints this outermost layer is column longitudinal reinforcement that passes through the joint. Damage State 11 is characterized by crushing of joint core concrete; joint core concrete is concrete within the outer most layer of joint reinforcing steel.

Researchers often do not report the extent of concrete spalling and crushing; however, these data can often be determined from review of the pictures of damaged components that are provided. This method of determining the extent of concrete crushing and spalling introduces uncertainty into the process in two ways. First, planar cracks may develop in cover concrete but cover concrete may not become detached and fall from the specimen. This concrete is referred to here as "flaked concrete." Some researchers will remove this concrete, with the result that the concrete becomes spalled concrete, and the specimen, for the purposes of this study, is considered to have reached a higher damage state. However, some researchers will not remove this concrete, with the result that the specimen is not considered to have achieved a high damage state. Second, in many cases, determination of the extent of spalling is done using pictures provided by the researchers. These pictures typically are not high resolution and may not be high quality; thus, some information is lost. Additionally, since evaluation of pictures is done by the research team, this necessarily introduces some interpretation error into the study.

3.4.1 Damage State 6

Damage State 6 defines the transition from cracking to spalling. Cracking is no longer measurable where the smooth surface has broken and fallen away. Spalling begins in the center of the joint and must cover to an area of 10% of the joint surface area. This amount of damage to the surface area means crack widths can not be measured. Figure 3.4 is an example of the small area of exposed aggregate surrounded by flaked sections of cover concrete.

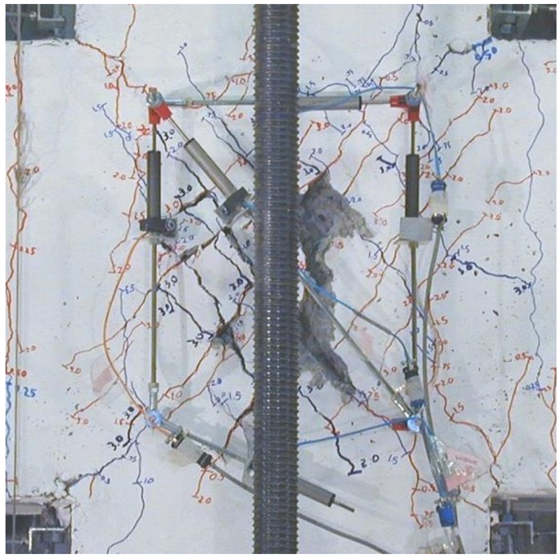

Figure 3.4 Joint Specimen PEER 22 exhibits Damage State 6 (Walker 2001)

3.4.2 Damage State 8

Damage State 8 describes spalling of more than 30% of the joint surface area. Thicker sections of cover concrete break and fall away from the center of the joint exposing the center column longitudinal reinforcement. At the same time, the area of exposed aggregate grows bigger but remains concentrated in the center of the joint surface. The amount of surface area exposed is important for the application of the MOR. Figure 3.5 provides an example of a joint that has reached Damage State 8.

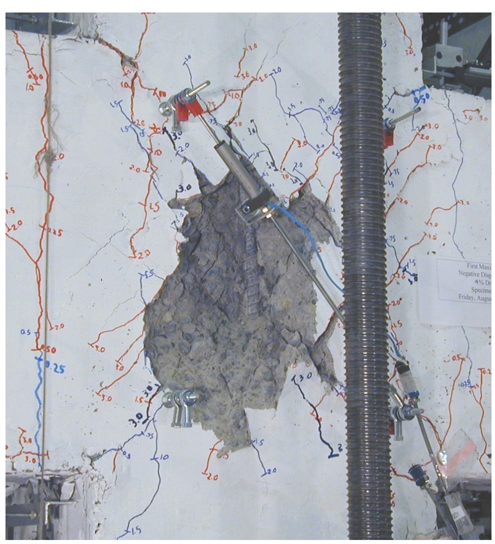

Figure 3.5 Joint Specimen PEER 14 exhibits Damage State 8 (Walker 2001)

3.4.3 Damage State 10

Damage State 10 defines spalling of more than 80% of the joint surface area. Both the depth and the width of the area of spalling continue to grow, exposing the corner column longitudinal reinforcement. Spalling that exposes the column longitudinal reinforcement may require removal and recasting of the joint core concrete to ensure that column bar bond capacity within the joint is not compromised.

3.4.4 Damage State 11

Damage State 11 defines crushing of the concrete extending into the joint core. Spalling of more than the cover concrete is considered crushing. Breaking and falling away of concrete thicker than the cover leads to exposure of the interior aggregate and large sections of the rebar (Fig. 3.6). The steel reinforcement is in danger of damage where no concrete is present to prevent buckling.

Figure 3.6 Joint Specimen C15 14 exhibits Damage State 11 (Walker 2001)

3.5 JOINT FAILURE MECHANISMS

Damage States 12(a, b, c) define three types of failure commonly observed in older reinforced concrete joints. Despite the numbering, these states are not progressive but would occur for the same high earthquake loads. These failure mechanisms should be expected where the design details of these joints do not confine the joint core. The first, and most common among the selected joints, is the buckling of the longitudinal steel reinforcement. Plastic deformation or hinging of the beam, rather than the joint or the column, is the current design target. However, damage to joints may not allow transfer of the stresses into the beam and result in movement within the joint.

3.5.1 Damage State 12(a)

Damage State 12(a) is the failure due to loss of gravity-load capacity within the joint. Inevitable after crushing of the core concrete, only the longitudinal reinforcement is available to resist the gravity load. During or even after the earthquake motion has ceased, buckling of the rebar occurs (Fig. 3.7).

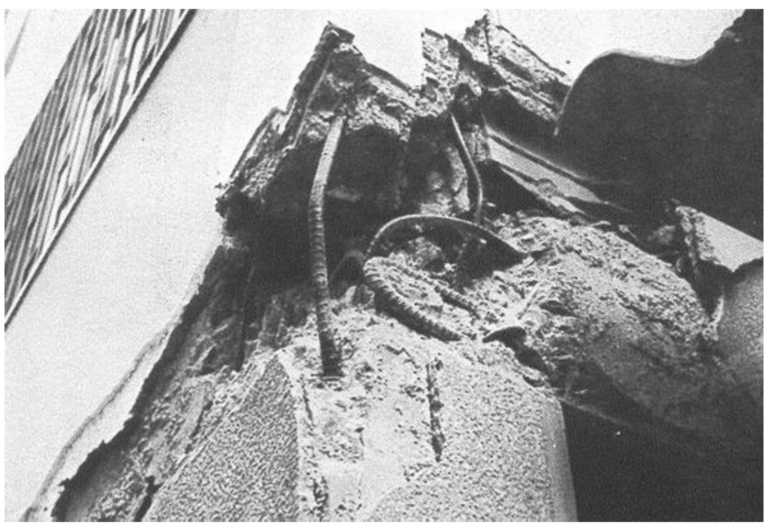

Figure 3.7 Exterior joint exhibiting Damage State 12 (PCA 1967)

3.5.2 Damage State 12(b)

Damage State 12(b) is defined as the loss of beam longitudinal steel anchorage with the joint. The beam appears to pull away from the joint and move without resistance against the lateral loading. The bond between the beam and the joint is lost when a significant amount of the concrete is crushed. Interior joints, Specimens J-B1, P4, and P3 all exhibit this failure. Pessiki et al. (1990) describe this damage state, “The north beam [of Specimen P3] pulled away from the beam-column joint, pivoting about [a large] crack and offering decreasing resistance with increasing displacement."

3.5.3 Damage State 12(c)

Reinforcement details of some interior joint specimens reveal that the beam longitudinal reinforcement is noncontinuous through the joint. The rebar ends are embedded only 6 in. into the joint. Like the previous damage state, Damage State 12(c) defines bond failure for these embedded specimens. Pessiki et al. (1990) describe this damage state, "Failure [of Specimen P9] was attributed to pullout of the embedded positive beam reinforcement from the beam-column joint, accompanied by significant damage to the top and bottom columns."

3.6 STRENGTH-BASED DAMAGE MEASURES

Strength-based damage is measured using instrumentation or measurement techniques that are available only in the laboratory. Inclusion of the DSs is influenced by the damage progression chronicled by Zhang and Jirsa (1982). Zhang and Jirsa note that as the loading increases toward the point of joint failure "deformation [of joint core concrete] reaches a value that corresponds to the ultimate strength of concrete under compressive loading." This point precedes joint failure, suggesting that there is a point at which damage can not be observed externally but at which the onset of significant damage and failure is inevitable. Assuming that the same point exists for joint failure, a state must be defined for the onset of significant shear damage as well as significant bond damage. This becomes especially important when the previous DSs are not described in the study or the loading is halted before failure. The Damage States 4 and 7 provide additional information where other damage descriptions are insufficient.

3.6.1 Damage State 4

Damage State 4 is yielding of the beam longitudinal reinforcement. The results of previous research suggest that after reinforcing steel yields, the strength of the concrete-steel bond is reduced. This is because the Poisson effect, which causes the diameter of the bar to decrease under tensile loading, becomes significant in the post-yield regime. With reduced bond capacity, the slip between the concrete and the reinforcing steel within the joint is increased and there is a redistribution of loading within the joint core. Ultimately this may result in increased damage within the joint.

3.6.2 Damage State 7

Damage State 7 is the onset of shear strength degradation. The shear capacity of the joint will reach a maximum and begin to deteriorate before the joint is assumed to have lost integrity and failed. Maximum joint strength may be identified using the load-displacement history for the joint subassemblage; these data typically are reported by all researchers. For the current study, the onset of shear strength degradation is defined as occurring when the maximum load during the next load cycle for which the displacement demand exceeds the current displacement demand is *significantly less* than of the current strength. For most specimens, significantly less strength was defined as less than 80% of the current strength. The data in Figure 3.8a show a column shear versus drift history for a specimen (Specimen P8 tested by Pessiki et al. (1990)) that exhibits more than a 20% drop in capacity between subsequent cycles. The data in Figure 3.8b show a column shear versus drift history for a specimen (Specimen P7 tested by Pessiki et al. (1990)) that exhibits a significant loss of capacity that is less than 20% between subsequent cycles. Both of these specimens are considered to exhibit Damage State 7. Figure 3.9 shows a specimen (Specimen P4 tests by Pessiki et al. (1990)) that is not considered to have achieved Damage State 7. The cycle at which peak shear capacity is developed is followed by one cycle of nearly the same capacity. Then, the test is terminated due to Damage State 12(b), beam pulling away from the joint.

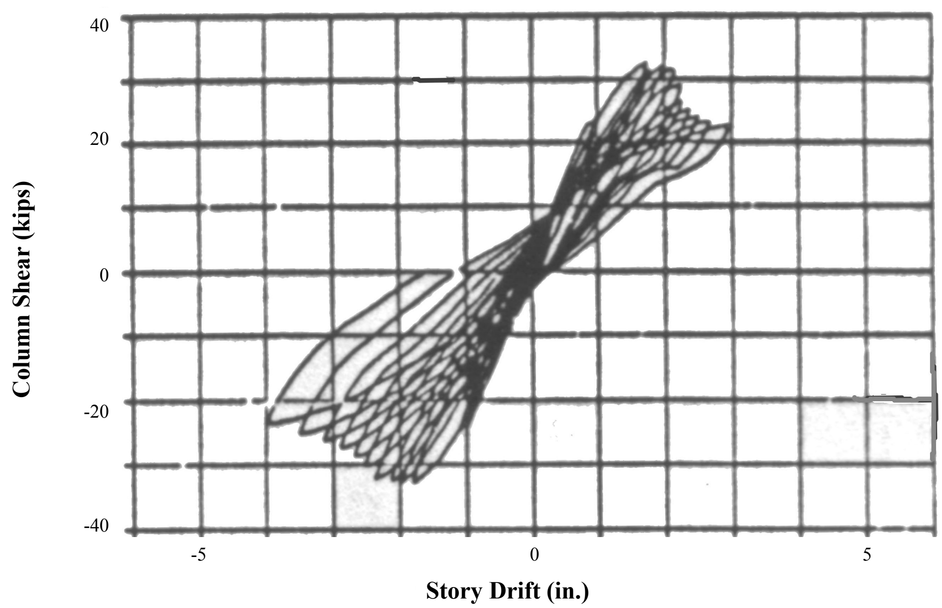

(a) Specimen P8 tested by Pessiki et al. (1990)

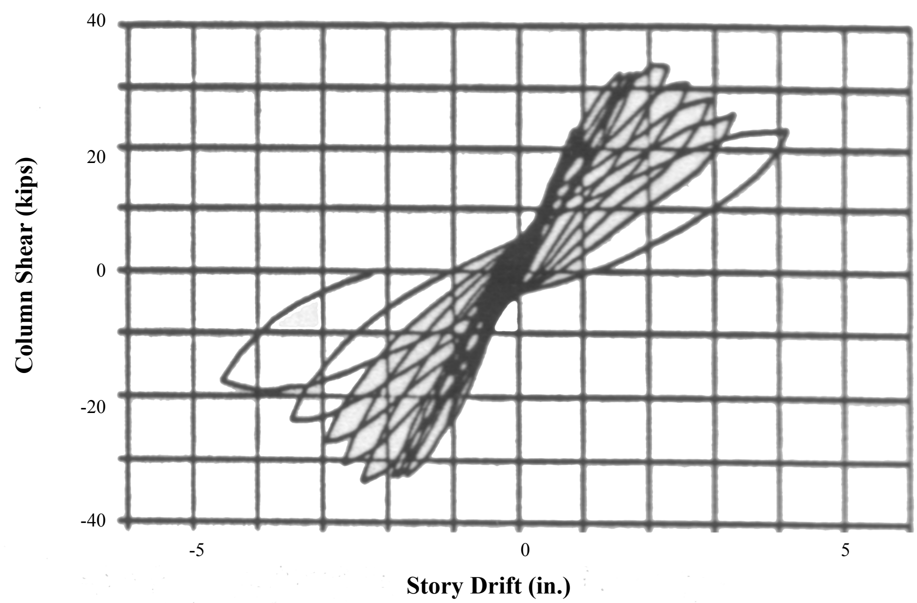

(b) Specimen P7 tested by Pessiki et al. (1990)

Figure 3.8 Specimens exhibiting Damage State 7

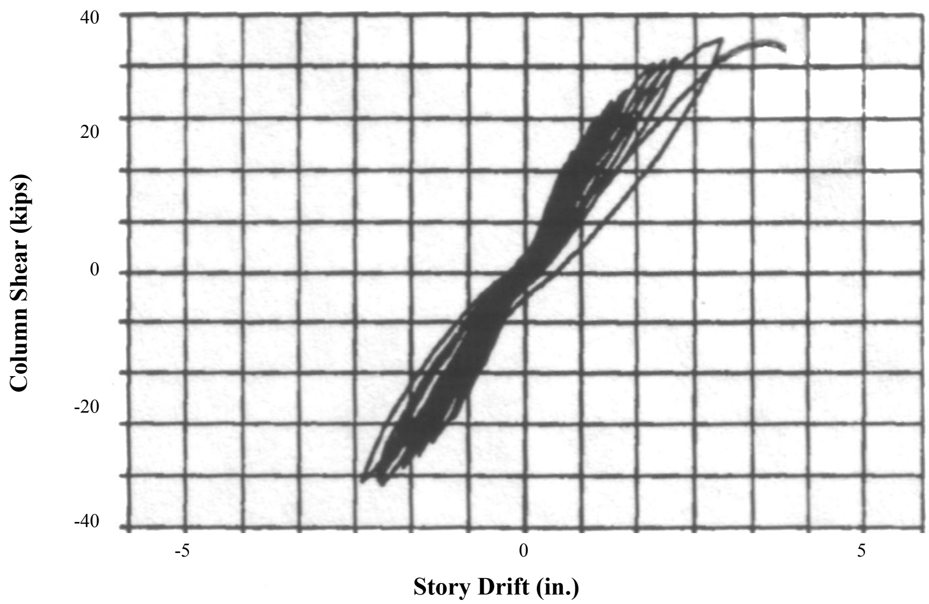

Figure 3.9 Specimen P4 tested by Pessiki et al. (1990) that does not exhibit Damage State 7

3.7 CONCLUSION

The selected experimental studies describe the damage sustained by joints subjected to earthquake loading. The damage measures are defined in terms of cracking, crushing, and joint failure. Six DSs characterize the location and width of the cracks. Investigation of current repair techniques identifies the widths significant for repair. Four DSs characterize the amount of concrete spalled and crushed within the joint. Two strength-based DSs are not visually observable but are strong indication of damage. Three types of joint failures are described for different types of beam bar detailing.

4 Engineering Demand Parameters and Experimental Data

4.1 INTRODUCTION

Engineering demand parameters (EDPs) define the earthquake demand for component-specific behavior. Investigation of the EDPs used commonly in seismic modeling determines the best EDP for the modeling of beam-column joints based on the data gathered from previous experiments. EDPs are linked to the DMs by probability models calibrated using this experimental data. Thus, identifying the appropriate EDPs represents the second phase in developing models for use in predicting the economic impact of earthquake-induced damage.

This chapter discusses the EDPs considered for use in predicting required repair associated with earthquake-induced damage in older beam-column joints. Section 4.2 discusses collection of EDP-DS data. Section 4.3 defines the engineering demand parameters appropriate for the seismic response of beam-column joints.

4.2 EXPERIMENTAL DATA

The results of previous experimental investigations are used to generate EDP-DS data sets that form the basis for development of the probabilistic MOR models. As discussed in Section 2.3, the beam-column joint test specimens from which data were collected from this study were chosen because (1) they were representative of pre-1967 construction, (2) they were representative of interior joints in two-dimensional frames, and (3) sufficient data were provided documenting damage patterns and the progression of damage during testing.

In collecting the EDP-DS data, the results of the experimental investigation were reviewed to determine the value of the EDP at the point during the load history where a specific level of damage was observed by the research team to be reached or exceeded. Typically, in performing experimental testing of structural components, testing is paused only intermittently to evaluate and document damage. Thus, tremendous uncertainty is introduced into the model development process because the value of the EDP associated with meeting a specific level of damage is, in actuality, only the value of the EDP at which the laboratory researchers *observed* that a particular level of damage had been achieved. The true value of the EDP at which the damage was reached could be any value in excess of the previous point at which testing was paused to assess damage, and it was observed that the particular level of damage had not been exceeded.

Figure 4.1 shows points on a joint shear stress versus shear strain history provided by Walker (2001) at which DSs, identified in Chapter 2, are observed by the research to have been reached. These points are associated with peaks in the shear strain history because testing was paused at maxima and minima in the displacement history to evaluate and document damage.

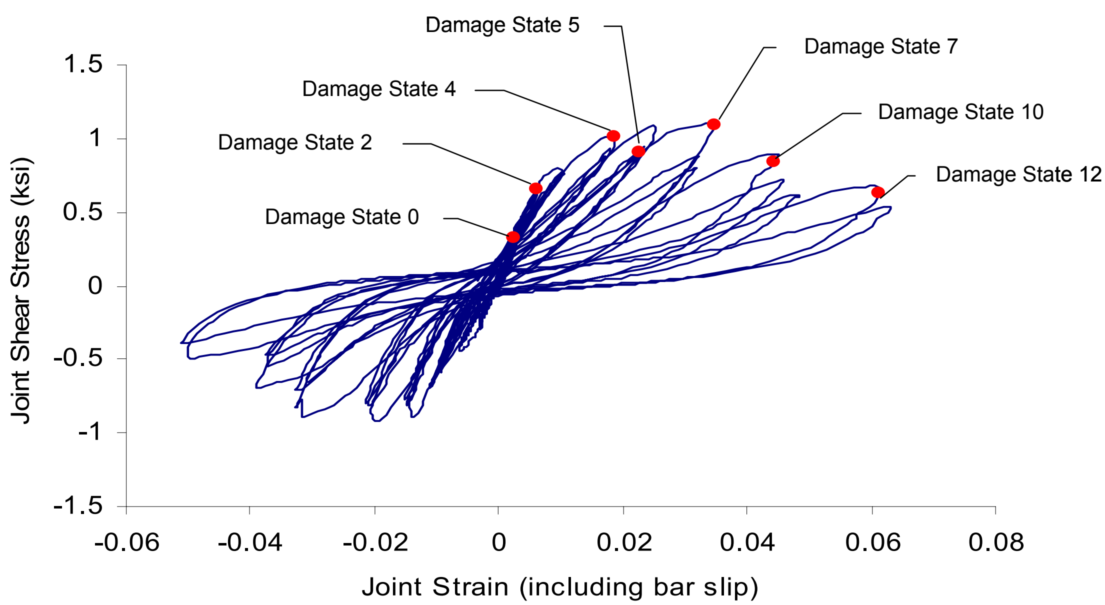

Figure 4.1 Damage states are identified on the response history for Specimen PEER 22 (adapted from Walker 2001)

4.3 ENGINEERING DEMAND PARAMETERS

Review of previous research results in the identification of five potential EDPs for use in predicting joint damage and required repair: maximum historic interstory drift, number of load cycles, maximum historic joint shear strain, a nonlinear function of drift and number of load cycles, and a nonlinear function of joint shear strain and number of load cycles. The value of the

EDP at any point on the load history is computed using the data provided by the researchers; joint shear strain is provided only by the researchers from UW (Walker 2001, Alire 2002).

4.3.1 Drift Ratio

Interstory drift ratio is a simple and commonly employed measure of the earthquake demand on structural components. For beam-column building joint subassemblages, the ratio may be computed from the data typically reported by researchers.

Figure 4.2 shows two commonly employed test configurations for building joint subassemblages; both configurations result in identical loading of the joint. Given the load configuration shown in Figure 4.2a, interstory drift is computed as

$$drift = \frac{\Delta_c}{\ell_{column}} \times 100 \tag{4.1}$$

where ℓ_{column} is the total length of the continuous column segment shown in Figure 4.2a and the factor of 100 is included so that drift defines a percentage. Given the load configuration shown in Figure 4.2b, interstory drift is computed as

$$drift = \frac{2\Delta_b}{\ell_{beam}} \times 100 \tag{4.2}$$

where ℓ_{beam} is the total length of the continuous beam segment shown in Figure 4.2b and the factor of 100 is included so that drift defines a percentage.

Most of the experimental test programs from which data were collected for the current study employed loading under displacement control with a displacement history comprising three complete displacement cycles to monotonically increasing maximum displacement demands (Table 2.2 identifies the displacement history employed in the test). In this case, approximately the same displacement demand is imposed in positive and negative loading, for the tests conducted by Pessiki et al. (1990), the researchers recommend that the "maximum displacement demand" be computed as the average of the absolute value of the maximum and minimum displacement demand imposed on the system for any particular load cycle. The approach is used in defining the maximum historic drift for the Pessiki test specimens.

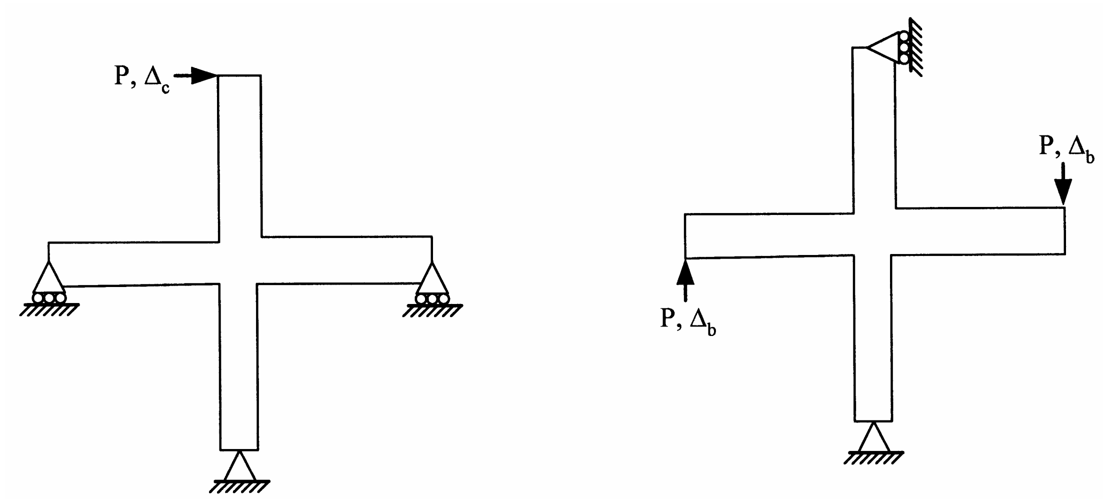

(a) Shear Load Applied to Column **(b) Shear Load Applied Beams**

Figure 4.2 Boundary conditions for beam-column joint subassemblage tests

4.3.2 Number of Cycles

Damage indices developed in the past suggest that the number of cycles may be an indicator of damage. The number of cycles is representative of the energy dissipated by the component. The results of experimental testing of reinforced concrete components suggest that cyclic loading to displacement demands that are less than the historic maximum displacement demand is less damaging. Thus, in counting cycles for arbitrary displacement histories, it is appropriate that cycles to displacement demands that are larger than the maximum historic displacement demand have more weight than cycles to displacement demands that are smaller than the maximum historic demand. To accomplish this, the cycle-counting algorithm proposed by Lowes (1999) is used in the current study. This algorithm defines the cycle counts as shown in Equation 4.3

$$\sum_{i=1}^{n} \frac{|\Delta u_i|}{4u_{\max}} \tag{4.3}$$

where the u_{max} is the maximum historic displacement demand, Δu_i is the current displacement increment and n is the number of displacement increments. This algorithm weighs cycles on the basis of the ratio of maximum displacement demand of the cycle to the maximum historic displacement demand.

The cycle-counting algorithm defined by Equation 4.3 was developed for use in nonlinear analysis with incrementally advancing solution algorithms. For the current study it is possible to consider displacement increments that are one quarter of a complete cycle; thus Equation 4.3 is modified to

$$\sum_{i=1}^{n}\left|\frac{(u_{hc})_i}{2u_{\max}}\right| \tag{4.4}$$

where u_{hc} is the maximum displacement of a half cycle and n is the number of half-cycles.

Applying the algorithm defined in Equation 4.4 to a traditional displacement history in which the maximum specimen is subjected to three cycles each to monotonically increasing maximum displacement demands results in a cycle count exactly equal to the number of displacement cycles imposed. Applying the algorithm to an arbitrary load history, such as that shown in Figure 4.3, results in a cycle count that is less than the number of complete displacement cycles, assuming that all cycles are weighted equally. For example, the cycle count for the entire history shown in Figure 4.3 is 7.

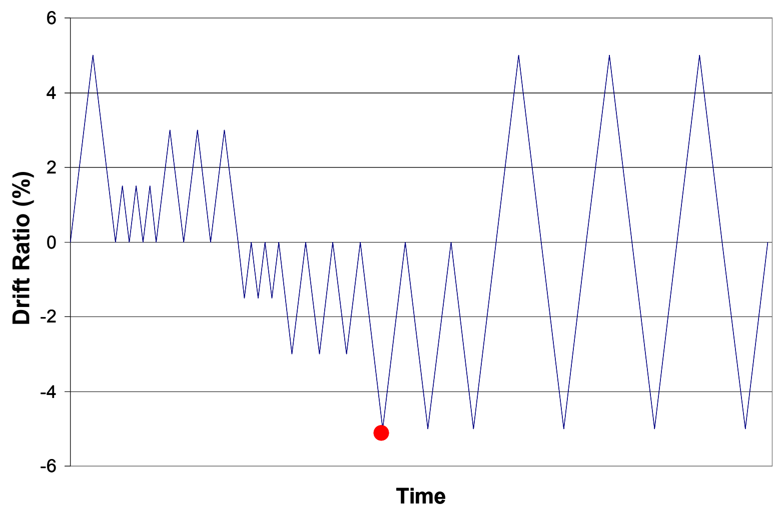

Figure 4.3 Drift history for PADH 14 as presented by Walker (2001)

4.3.3 Joint Shear Strain

Joint shear strain defines the deformation demand imposed only on the joint. Interstory drift is the summation of beam flexural and shear deformation, column flexural and shear deformation and joint deformation. Since joint shear strain is a measure only of joint demand, it could be expected to be a more efficient predictor of joint damage.

In the laboratory, joint shear strain typically is measured using multiple linear variable differential transformers (LVDT) embedded in the joint concrete. Figure 4.4 shows an LVDT configuration that could be used to measure joint shear. Of the experimental test programs considered in the current study, only the tests by Walker (2001) and Alire (2002) measured joint shear deformation. In these tests, two sets of LVDTs were used to measure shear, one that included approximately 80% of the joint surface area (Figure 4.4) and one than included substantially less of the joint area (not shown in Figure 4.4; these instruments were placed on the back side of the specimen shown in Figure 4.4). Data from the larger of the two LVDT configurations were used in the current study, as recommended by Walker (2001) and Alire (2002).

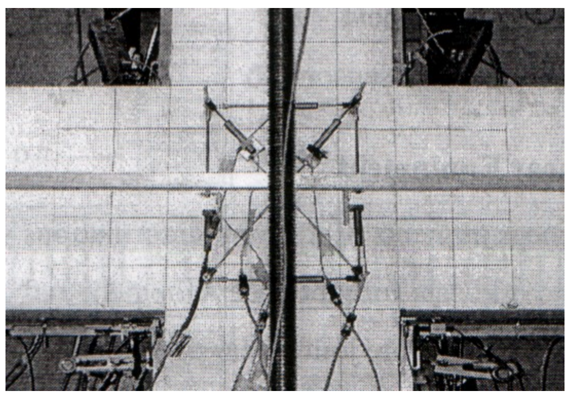

Figure 4.4 Joint strain is measured by the large shear rig (Alire 2002)

4.3.4 Nonlinear Function of Drift and Cycles

The results of previous research suggest that a functional EDP that defines demand on the basis of both maximum historic interstory drift and number of load cycles may be a more efficient predictor of damage. Using this type of EDP, the impact of both displacement demand and energy dissipation are included. For the current study, a simple nonlinear function was considered

$$F = aD^b + cN^d \tag{4.5}$$

where D is the maximum historic interstory drift and N is the number of load cycles, and empirical coefficients are defined a=0.252, b=0.645, c=0.0178, and d=0.819. The coefficients *a, b, c,* and *d* were computed to reduce the scatter of the damage data about a line ranging from F=0 to F=1.

4.3.5 Nonlinear Function of Shear Strain and Cycles

A nonlinear function that combines the maximum historic joint shear strain and the number of load cycles also could be expected to be an efficient predictor of joint damage. In the current study, a nonlinear function similar to that used for combining drift and number of load cycles (Eq. 4.5) was considered

$$F = a\gamma^{b} + cN^{d} \tag{4.6}$$

with γ equal to the maximum historic joint shear strain, N equal to the number of shear-strain cycles and empirical parameters defined as follows: a = 1.46, b = 0.481, c=0.200, d = 0.309. As with Equation 4.5, the empirical model parameters are computed to minimize scatter about a line ranging from F=0 to F=1.

4.4 CONCLUSION

The results of previous experimental investigations of the earthquake response of beam-column joints were evaluated to identify a series of EDPs for use in predicting this damage. Five EDPs were considered for use: maximum historic interstory drift, the number of displacement cycles, the maximum historic joint shear strain demand, a nonlinear function of drift and number of cycles, and a nonlinear function of joint shear strain and number of cycles. Interstory drift is provided by all researchers; however, this measure of joint demand includes the influence of the beam and column inelastic deformation. Joint shear strain could be expected to provide an improved measure of the earthquake demand on the joint; however, these data are provided by very few researchers. The nonlinear functions provide a means of capturing the impact of both deformation demand and number of load cycles.

5 Methods of Repair

5.1 INTRODUCTION

This chapter defines a series of progressively extensive repair techniques that can be used to restore a damaged reinforced concrete structural component to its original, pre-earthquake strength and ductility capacity. Given a required MOR, the cost associated with completing that repair as well as the time required to complete the repair, which in combination define the economic impact of the earthquake damage, can be estimated using traditional cost-estimating techniques. The repair techniques considered in the current study are included in the repair documentation identified in Section 2.4 and have been used in the field following recent earthquakes on the West Coast of the United States.

The proposed repair techniques are organized into five MORs progressing from the most minimal type of repair, Method of Repair 0: Cosmetic Repair, to the most substantial, Method of Repair 4: Replace Joint. The MORs are assumed to be comprehensive and mutually exclusive, though the same repair activities are included in more than one MOR. Given the damage state sustained by a component, the information presented in this chapter links damage to repair to enable the progression from component damage to economic loss.

5.2 LINKING REPAIR WITH DAMAGE

The MOR required to restore a component to its original, pre-earthquake condition, provides a basis for estimating the economic impact of earthquake loading. Information from multiple sources is used to identify appropriate techniques for repairing earthquake damage to RC components and to link these repair methods with the range of previously identified DSs. The primary references consulted for this study were *FEMA 308 Repair of Earthquake Damaged Concrete and Masonry Wall Buildings* (1998) and *ACI 546R-96 Concrete Repair Guide* (1996). In addition, the results of previous research by others were used to verify the adequacy of repair methods and to identify which repair methods would be employed for which DSs (Jara et al. 1989, Karayannis 1998, Filiatrault 1996, Tasai 1992, French et al. 1990). Additionally, practicing engineers and contractors were consulted to verify linkages between repair methods and DSs (Coffman and Kapur 2003, Runacres 2003, Savage 2003).

Review of the relevant references resulted in identification of five MORs that would be appropriate for restoring joints to their original condition (Table 5.1). These MORs include five basic repair techniques: repair cosmetic finishes, epoxy inject concrete cracks, patch spalled concrete, remove and replace crushed concrete, replace reinforcing steel. Review of the relevant references also provided a basis for linking these MORs with specific DSs (Table 5.1). While the probabilistic framework employed for prediction of economic impact (Fig. 1.1 and Eq. 1.1) would suggest that there should be a probabilistic relationship linking each repair method with a set of DSs, there are insufficient data available to calibrate such models.

Table 5.1 Damage states assigned to each repair technique

Method of Repair	Activities	Damage States
0. Cosmetic Repair	Replace and repair finishes.	0-2
1. Epoxy Injection	Inject cracks with epoxy and replace finishes.	3-5
2. Patching	Patch spalled concrete, epoxy inject cracks and replace finishes.	6-8
3. Replace Concrete	Remove and replace damaged concrete, replaces finishes	9-11
4. Replace Joint	Replace damaged reinforcing steel, remove and replace concrete, and replace finishes.	12

5.3 METHOD OF REPAIR 0: COSMETIC REPAIR

If component damage due to earthquake loading is limited to concrete cracking with narrow crack widths, the impact on component strength and stiffness will not be significant and repair will not be required to restore the component strength and stiffness to pre-earthquake conditions. However, concrete cracking may allow for water infiltration into the wall, impair fire resistance, or result in damage to surface finishes. Thus, limited concrete cracking requires repair or replacement of surface finishes.

Method of Repair 0 comprises activities to remove, repair and/or replace surface finishes, and is equivalent to Cosmetic Repair 1 defined in *FEMA 308* (1998). These activities may include plastering, taping, painting, and replacing wallpaper, as well as the application of coatings and sealants to reduce permeability and/or improve fire resistance. These activities are not intended to improve the strength or stiffness of the component.

Discussions with structural engineers and contractors indicate that the extent of damage that an owner considers to require repair of surface finishes is highly variable. For the current study, this MOR is linked with Damage States 0 and 1; this is considered to represent a conservative estimate of repair requirements. Additionally, this MOR is linked with Damage State 2, defined by a maximum concrete crack width of 0.02 in. As discussed previously, this residual crack width, which was used as a limit for requiring repair following the Mexico City earthquake (Jara 1989), is somewhat in excess of the limits recommended by older versions of the ACI Building Code (1995) and somewhat more conservative than the limits that have been employed in the field.

5.4 METHOD OF REPAIR 1: EPOXY RESIN INJECTION OF CRACKED CONCRETE

If earthquake damage results in significant opening of concrete cracks, repair may be required to restore component stiffness and strength as well as to ensure that earthquake damage does not make the component vulnerable to water infiltration, corrosion, and fire damage. Injection of cracks with an epoxy resin or a cementitious grout is a commonly employed repair method for reinforced concrete components damaged under multiple types of loading, including earthquake loading. Two methods are typically used to introduce epoxy into cracks: pressure injection in which epoxy is injected under pressure into ports that are drilled into cracks at various locations, and vacuum impregnation in which epoxy is introduced into cracks at one location and a vacuum is created at another location to pull the epoxy into the cracks (ACI 1999). Cracks with widths ranging from 0.002 in. to 0.75 in. may be repaired using epoxy injection. This MOR is comparable to Structural Repair 1 defined in *FEMA 308* (1998).

The results of multiple laboratory investigations indicate that epoxy injection can restore component strength and stiffness to levels that are comparable to pre-earthquake conditions. For example, Filiatrault (1992) subjected an exterior building joint to simulated earthquake loading to a maximum drift demand of 1.4%, resulting in yielding of beam longitudinal reinforcement, repaired the joint using epoxy injection, applied simulated earthquake loading, and found the joint to have strength and stiffness properties comparable to original conditions. Additionally, French et al. (1990) subjected interior beam-column joints with high bond-stress demands to cyclic lateral loading to maximum interstory drift levels of 3%, repaired the joints using both pressure injection and vacuum impregnation techniques to introduce epoxy into concrete cracks, and observed that the repaired joints had lateral stiffnesses that exceeded 85% of the original stiffness, lateral strengths approximately equal to the original strength and energy dissipation capacities, for critical drift cycles, that exceeded 85% of the original energy dissipation capacity.

In linking epoxy resin injection with DSs, identifying the crack widths for which epoxy injection is an appropriate repair method is the critical issue. As discussed previously, maximum concrete cracks with width exceeding 0.02 in. (Damage State 3) are considered to require this MOR.

5.5 METHOD OF REPAIR 2: PATCHING OF SPALLED CONCRETE

Under moderate to severe earthquake loading, damage may include spalling of the surface concrete. In this case, replacement of the spalled concrete is required to restore the strength and stiffness provide by this concrete as well as to ensure that reinforcing steel, possibly exposed by spalling of the concrete, is not vulnerable to corrosion, fire damage, etc. Patching is accomplished by removing any loosened, damaged concrete that has not spalled, cleaning the surface, and replacing the concrete with a mortar mix that includes sand, pea gravel and either an inorganic base material, such as Portland cement or latex-modified concrete, or an organic base material, such as epoxy or polyester (FEMA 308). Method of Repair 2 includes only removal of detached, but not spalled concrete, epoxy injection of cracks and patching of concrete. It does not include a significant effort to remove damaged and undamaged concrete. Method of Repair 2 includes some of the activities identified in Structural Repair 3 in *FEMA 308* (1998).

The results of previous research indicate that patching of spalled concrete using a cementitious material is an appropriate repair technique to restore the strength and stiffness of components exhibiting spalling of cover concrete. For example, Karayannis (1998) repaired an exterior joint that exhibited spalling using a cement paste with low shrinkage, high compressive and tensile strength, rapid hardening properties, and adhesion properties that were enhanced by the addition of an adhesive to the paste. The repair joint exhibited strength and stiffness comparable to original, pre-earthquake conditions.

In linking Method of Repair 2 with the previously defined DSs, the critical issue is to identify the extent of concrete spalling for which patching of spalled concrete is inadequate and, thus, the damage level at which more extensive repair is required. Discussions with engineers and contractors as well as consideration of bond-zone conditions resulted in the decision that if a substantial area of joint core concrete has spalled, resulting in exposure of most or all of the column longitudinal reinforcement, then patching of the spalled concrete is not sufficient. If a large surface area of concrete has been lost and all of the column longitudinal reinforcement has been exposed, simply patching the spalled concrete will not be adequate to restore bond capacity for column longitudinal steel and, thus, will not be sufficient to restore strength and stiffness to pre-earthquake conditions. For this reason, Method of Repair 2 is linked with Damage States 6, 7 and 8.

5.6 METHOD OF REPAIR 3: REMOVAL AND REPLACEMENT OF DAMAGED CONCRETE

If spalling of cover concrete is extensive, concrete damage extends to crushing of the joint core concrete, or crack patterns suggest that anchorage failure has occurred within the joint, it may be necessary to remove and recast joint concrete. Method of Repair 3 is an expansion of the activities included in Method of Repair 2 and includes removal and replacement of damaged and potentially damaged concrete. In removing concrete, the objective is to ensure that only undamaged concrete remains as well as to ensure that a substantial volume of new material is placed around beam and column reinforcement to ensure that full bond capacity is recovered. Typically, the replacement material will be a standard concrete mix including sand and coarse aggregate. If more than 6 in. of concrete thickness is removed, mechanical anchorage devices, such as epoxy-embedded dowel bars, are recommended to ensure bond between new and existing concrete (*FEMA 308* 1998, *ACI 546R* 1996). Method of Repair 3 differs from Method of Repair 2 in that (1) chipping or jack-hammering is used to remove all potentially damaged concrete and (2) typical concrete mixes may be used. If substantial concrete is removed from the joint region, it likely will be necessary to shore the structure and redistribute gravity away from the joint.

As discussed previously, the damage state at which replacement of joint concrete is required is determined primarily by exposure, and thus the potential loss of anchorage strength, of a significant portion of the column longitudinal reinforcement. Review of experimental data indicates that this occurs if concrete has spalled from 80% or more of the joint surface area. Thus, Method of Repair 3 is required for Damage States 9, 10, and 11.

5.7 METHOD OF REPAIR 4: REMOVAL AND REPLACEMENT OF DAMAGED REBAR

Under severe earthquake loading, column longitudinal reinforcement, exposed as a result of concrete crushing and spalling, may buckle under column axial load. If this occurs, the column reinforcement must be replaced using a mechanical connection. This type of repair may be appropriate also for continuous beam longitudinal reinforcement that has yielded due to substantial joint deformation or for discontinuous beam longitudinal reinforcement that has pulled-out of the joint.

Method of Repair 4 comprises the activities required to replace reinforcing steel. These activities include shoring the structure, removing concrete using chipping or jack-hammering, removing the damage sections of reinforcing steel, replacing the reinforcing steel, placing epoxy-embedded dowel bars as necessary and replacing joint concrete. Typically, new and existing reinforcing steel is connected using a mechanical connection such as sleeve, splice, or threaded coupler (*FEMA 308* 1998). Method of Repair 4 is comparable to Structural Repair 4 as defined by *FEMA 308* (1998).

Method of Repair 4 is required only if substantial yielding and/or buckling of beam or column reinforcement has occurred. Thus, Method of Repair 4 is linked with Damage State 12.

5.8 CONCLUSION

Five MORs were identified to restore the damaged joint to pre-earthquake condition; Cosmetic Repair, Epoxy Injection, Patching, Replace Concrete, and Replace Joint. These MORs include repair techniques that are specified commonly by structural engineers for repairing damage due to earthquake and other types of loading, that are employed commonly by contractors, that are documented in repair manuals, and that have been verified for use in repairing earthquake damage by experimental investigation. The results of previous research and the experience of structural engineers and contractors are used to associate, deterministically, each MOR with a set of DSs as identified in Chapter 3.

6 Predicting Repair as a Function of Demand

6.1 INTRODUCTION

Component-specific fragility functions provide the link between EDPs and the MOR required to restore a damaged component to pre-earthquake conditions. Empirical data link EDPs with DSs. Deterministic relationships between DSs and MORs extend these data to enable generation of EDP-MOR data sets. Standard probability models are calibrated to fit the EDP-MOR data. Section 6.2 presents the EDP-DS data, and Section 6.3 discusses the development of EDP-MOR data sets. Section 6.4 presents evaluation of the EDPs and identifies three preferred EDPs for use in predicting joint damage. Section 6.5 presents evaluation of the probability distributions using standard goodness-of-fit tests. Section 6.6 presents the proposed fragility functions.

6.2 DATA SETS

Experimental data characterizing the progression of damage for the test specimens were used to generate data sets linking the thirteen DSs with the three primary EDPs: drift, number of load cycles and joint shear strain. The functional EDPs, defined by Equations 5.2 and 5.3, were calibrated to minimize the dispersion of the data about a line extending through all of the DSs and spanning a range of functional EDP values from 0 to 1.0. Figure 6.1 shows the EDP-DS data for all of the EDPs. Visual inspection of the data in this figure suggests that the functional EDPs result in the least variability for each of the DSs and thus are the most efficient predictors of damage. Visual inspection suggests also that interstory drift is a more efficient predictor than number of load cycles or joint strain. In particular, load cycles and shear strain are problematic at low demand levels where a low demand may be associated with many, including relatively severe, DSs.

The scatter of the data in Figure 6.1 reinforces the need for probabilistic models linking EDPs with damage and repair. The variability in these data is due in part to variability in test specimen design and loading, as discussed in Section 2.3.3 as well as observation error as discussed in Chapter 3. However, the variability is due also to the tremendous uncertainty that is necessarily introduced as a result of experimental procedure. The typical procedure for conducting an pseudo-static experimental investigation of component response to earthquake loading is

1. A half-cycle of loading to a new maximum displacement demand, at which point loading is paused to allow for identification of new cracks and regions of spalling, measurement of new and existing cracks and picture taking.
2. Loading in the reversed direction to a new minimum displacement demand, at which point loading is paused to allow for data collecting as above.
3. Multiple additional full load cycles, typically two additional cycles, to the new maximum and minimum displacement demand levels.

Thus, in monitoring the progression of damage, it is not possible to know exactly the displacement demand level at which damage occurred, only that it occurred prior to reaching a particular maximum displacement demand level. Further it is not possible to differentiate between damage that occurs during the second cycle to a maximum displacement demand level from that which occurs during the third cycle or from that which occurs during the first cycle to an increased maximum displacement demand.

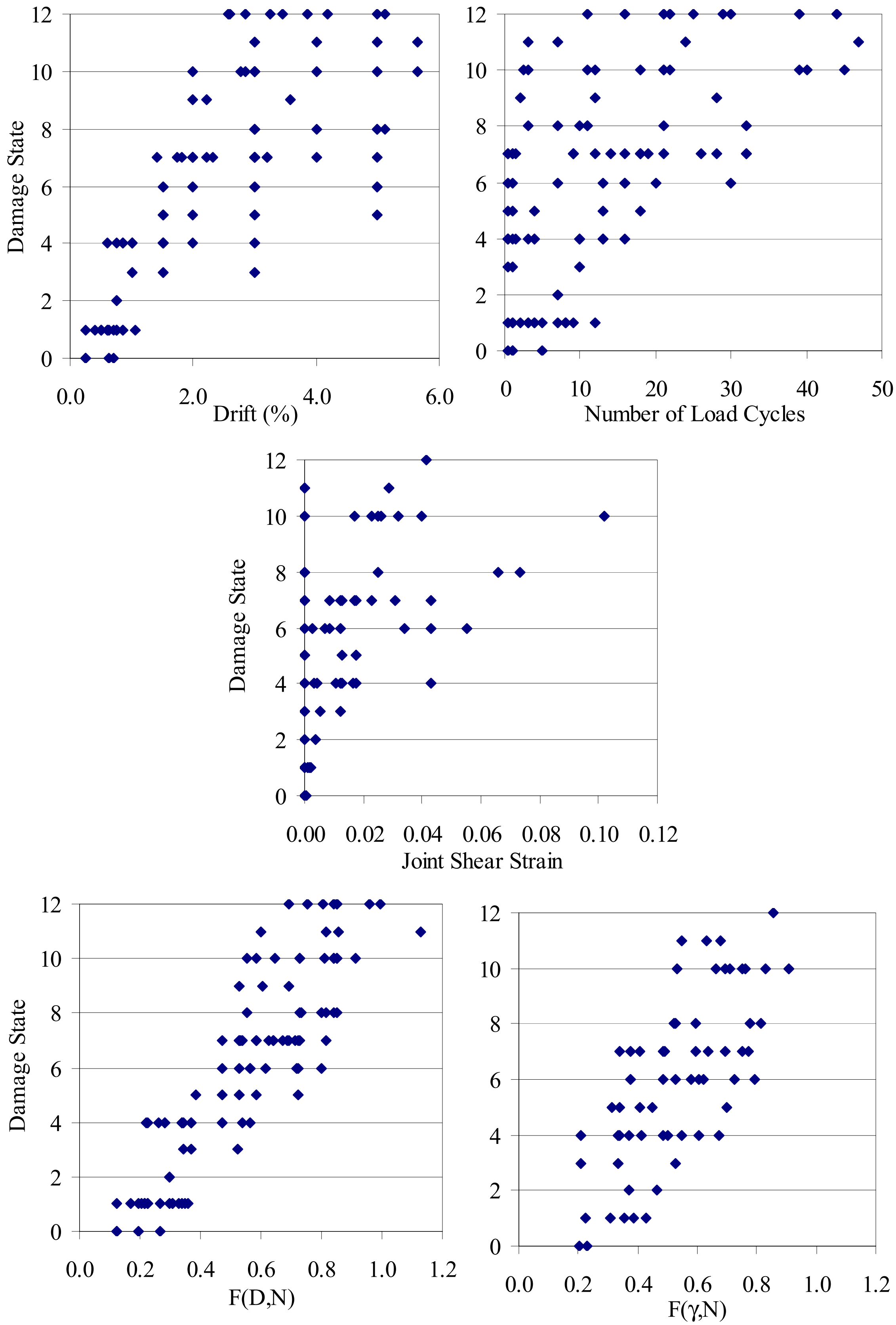

Figure 6.1 DS versus EDP

6.3 GROUPING DAMAGE DATA TO ENABLE PREDICTION OF REQUIRED REPAIR

The data presented in Figure 6.1 were used to develop models defining the probability of earthquake damage requiring, at least, the use of a specific MOR. These data could have been used to generate fragility curves defining the probability that joint damage would meet or exceed a specific damage state. However, this was considered unnecessary, since the ultimate objective of this effort was to develop tools to support the prediction of economic impact.

To generate the desired MOR prediction models, the data in Figure 6.1 were combined so that individual data points define a specific EDP value and the required MOR associated with that EDP value. This combination was accomplished using the relationships in Table 5.1. Because several DSs are linked with each MORs, there are several plausible approaches to combining the data:

- Method One: For each individual specimen, the EDP-damage state pairs are used for all of the damages state associated with a specific MOR. This method results in the most data points for each MOR, but also results in more dispersion and skews the MOR toward higher EDP levels.
- Method Two: For each individual specimen, the EDP-damage state pair for the lowest damages state associated with a specific MOR is used. This method results in no more than 21 data points for each MOR.
- Method Three: Only data for the lowest damage state are used for each MOR. This method results in the fewest data for each MOR.

Figure 6.2 shows the three combination methods for a single EDP, interstory drift.

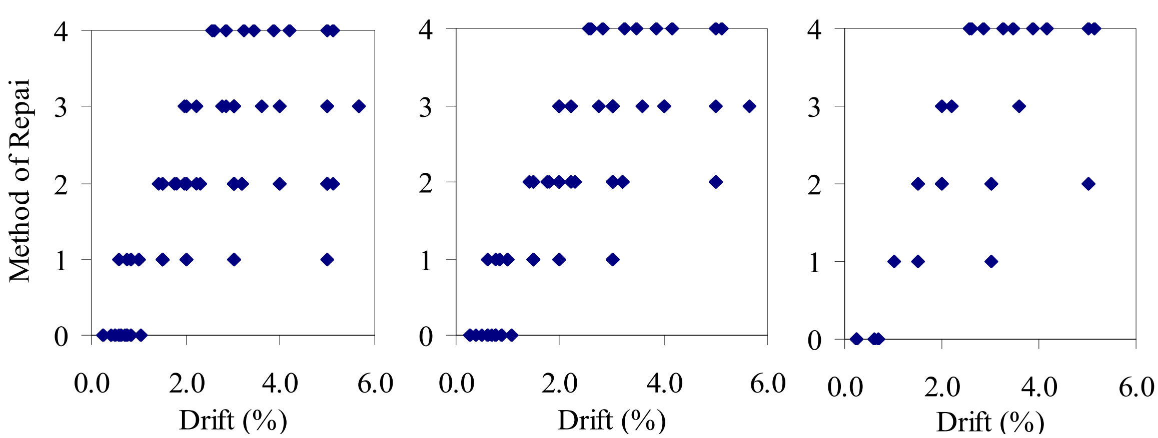

Figure 6.2 MOR versus drift with data combined using three proposed methods

6.4 EVALUATION OF THE PROPOSED EDPS

Given a specific value of an EDP, the ideal family of fragility functions results in identification of a single MOR that has a relatively high probability of being met or exceeded with all more extensive MORs having a relatively low probability of being met or exceeded. This requires that the EDP-MOR data have well-spaced means and low variances. **Table 6.1** shows the sample mean and coefficient of variation for each of the EDPs, MORs and damage-repair data combination methods. Several observations may be made regarding the data in **Table 6.1**:

- The functional EDPs result in the least variability of the data for each of the MORs and the most uniformly spaced means across the range of methods used to combine the DS data into MORs.
- Of the nonfunctional EDPs (maximum interstory drift, number of load cycles, maximum joint shear strain), drift result in the least variability of the data for each of the MORs and the most uniformly spaced means across the range of methods used to combine the DS data in MORs.
- Of the three methods proposed for combining the EDP-DS data to create EDP-MOR data sets, no single method is substantially superior to the others, though Method Three results in one MOR for which no data are available.

The first of these observations reinforces the visual observations made from the DS-EDP plots shown in Figure 6.1. On the basis of these data, combination Method Two was identified as the preferred data combination method for use in generating fragility functions. The coefficients of variation for Method Two are comparable to those of Method One, and Method Two has the advantage that for any specimen and any MOR only data for the lowest DS are used. Also, on the basis of the data presented in **Table 6.1**, three EDPs, maximum interstory drift, F(D,N) as defined by Equation 2, and $F(\gamma,N)$ and defined by Equation 3, are identified as the preferred EDPs and fragility functions are developed only for these EDPs.

Table 6.1 Characteristics of EDP-MOR data for the three data combination methods

	MOR	drift		no. of cycles		F(D,N) per Eq. 2		jt. Strain		F(γ,N) per Eq. 3	
		mean	c.o.v.	mean	c.o.v.	mean	c.o.v.	mean	c.o.v.	mean	c.o.v.
Data Combination Method One	0	0.6	0.33	4.7	0.69	0.25	0.30	9.84E-04	1.34	0.33	0.29
	1	1.7	0.61	5.7	1.04	0.41	0.32	1.03E-02	1.03	0.43	0.33
	2	3.0	0.38	13.8	0.72	0.65	0.17	2.14E-02	1.02	0.59	0.24
	3	3.5	0.33	19.9	0.75	0.75	0.20	2.67E-02	1.07	0.70	0.16
	4	3.7	0.26	26.3	0.40	0.83	0.12	4.15E-02	N.A.	0.86	N.A.
		max	0.61	max	1.04	max	0.32	max	1.34	max	0.33
		ave.	0.38	ave.	0.72	ave.	0.22	ave.	1.11	ave.	0.25
Data Combination Method Two	0	0.6	0.38	5.0	0.71	0.25	0.34	5.46E-04	1.05	0.29	0.34
	1	1.4	0.54	5.3	1.01	0.37	0.30	1.15E-02	1.11	0.44	0.30
	2	2.6	0.39	14.0	0.70	0.61	0.15	1.80E-02	1.08	0.56	0.23
	3	3.1	0.28	19.9	0.64	0.72	0.18	2.94E-02	1.03	0.71	0.17
	4	3.7	0.26	26.3	0.40	0.83	0.12	4.15E-02	N.A.	0.86	N.A.
		max	0.54	max	1.01	max	0.34	max	1.11	max	0.34
		ave.	0.37	ave.	0.69	ave.	0.22	ave.	1.07	ave.	0.26
Data Combination Method Three	0	0.5	0.53	1.9	1.12	0.18	0.40	1.52E-04	1.41	0.22	0.09
	1	1.8	0.57	3.8	1.39	0.41	0.23	5.91E-03	1.03	0.36	0.45
	2	2.9	0.50	12.9	0.77	0.62	0.18	2.03E-02	1.02	0.59	0.22
	3	2.6	0.34	14.0	0.94	0.61	0.14	N.A.	N.A.	N.A.	N.A.
	4	3.7	0.26	26.3	0.40	0.83	0.12	4.15E-02	N.A.	0.86	N.A.
		max	0.57	max	1.39	max	0.40	max	1.41	max	0.45
		ave.	0.44	ave.	0.92	ave.	0.21	ave.	1.15	ave.	0.25

6.5 SELECTION OF A STATISTICAL FUNCTION

The three standard probability functions were calibrated using the method of maximum likelihood to fit the EDP-DV data, with EDP-DS data combined following Method Two described in the previous section. The standard probability distributions were evaluated using the goodness-of fit tests discussed in Section 2.5.2. The results of these tests are shown in

Table 6.2 Results of $\chi 2$ and K-S tests for lognormal, Weibull, and beta distributions for the three preferred EDPs and the preferred damage data combination method

and 6.3. From the data in these tables, it may be concluded that the beta distribution does not provide as good a fit to the data as do the lognormal and Weibull distributions and that there is relatively little difference between the Weibull and lognormal distributions with respect to goodness of fit. Given these results, and that the lognormal distribution is more commonly used relative to the Weibull distribution, and that the Lilliefors test indicates the lognormal distribution to be correct for all but one case, the lognormal distribution was chosen as the preferred probability distribution for use in defining the fragility functions.

Table 6.2 Results of χ^2 and K-S tests for lognormal, Weibull, and beta distributions for the three preferred EDPs and the preferred damage data combination method

	Lognormal Distribution											
	Drift				F(D,N)				F(γ,N)			
	χ^2 Test		K-S Test		χ^2 Test		K-S Test		χ^2 Test		K-S Test	
MOR	Eq. 2.3	correct CDF	P	correct CDF	Eq. 2.3	correct CDF	P	correct CDF	Eq. 2.3	correct CDF	P	correct CDF
0	11.4	FALSE	0.32	TRUE	2.00	TRUE	0.65	TRUE	2.91	TRUE	0.65	TRUE
1	3.31	TRUE	0.65	TRUE	1.33	TRUE	0.74	TRUE	1.81	TRUE	0.94	TRUE
2	8.39	FALSE	0.61	TRUE	3.06	TRUE	0.87	TRUE	2.10	TRUE	1.00	TRUE
3	2.72	TRUE	0.63	TRUE	5.32	TRUE	0.61	TRUE	1.31	TRUE	0.97	TRUE
4	0.63	TRUE	0.99	TRUE	2.21	TRUE	0.88	TRUE	N.A.	N.A.	N.A.	N.A.

	Weibull Distribution											
	Drift				F(D,N)				F(γ,N)			
	χ^2 Test		K-S Test		χ^2 Test		K-S Test		χ^2 Test		K-S Test	
MOR	Eq. 2.3	correct CDF	P	correct CDF	Eq. 2.3	correct CDF	P	correct CDF	Eq. 2.3	correct CDF	P	correct CDF
0	5.70	TRUE	0.81	TRUE	0.75	TRUE	0.71	TRUE	3.10	TRUE	0.54	TRUE
1	4.42	TRUE	0.48	TRUE	1.89	TRUE	0.36	TRUE	1.02	TRUE	1.00	TRUE
2	7.30	FALSE	0.49	TRUE	1.41	TRUE	0.83	TRUE	2.93	TRUE	0.97	TRUE
3	4.02	TRUE	0.34	TRUE	6.01	FALSE	0.60	TRUE	0.69	TRUE	0.99	TRUE
4	1.03	TRUE	0.98	TRUE	2.70	TRUE	0.59	TRUE	N.A.	N.A.	N.A.	N.A.

	Beta Distribution											
	Drift				F(D,N)				F(γ,N)			
	χ^2 Test		K-S Test		χ^2 Test		K-S Test		χ^2 Test		K-S Test	
MOR	Eq. 2.3	correct CDF	P	correct CDF	Eq. 2.3	correct CDF	P	correct CDF	Eq. 2.3	correct CDF	P	correct CDF
0	4.91	TRUE	0.48	TRUE	0.32	TRUE	0.79	TRUE	22.5	FALSE	0.46	TRUE
1	2207	FALSE	0.15	TRUE	3.74	TRUE	0.40	TRUE	2.25	TRUE	0.60	TRUE
2	832	FALSE	0.05	FALSE	3.31	TRUE	0.83	TRUE	9.19	FALSE	0.86	TRUE
3	16.20	FALSE	0.64	TRUE	10.11	FALSE	0.29	TRUE	1.88	TRUE	0.90	TRUE
4	1.85	TRUE	0.77	TRUE	6.69	FALSE	0.78	TRUE	N.A.	N.A.	N.A.	N.A.

Notes: (1) For the K-S test, $P = P\left(D_n \le D_n^{\alpha}\right)$. (2) For all cases of the χ^2 test, the sum defined by Equation 6 is compared with $c_{1-\alpha,f} = 5.992$.

Table 6.3 Results of the Lilliefors test for the lognormal distributions for the three preferred EDPs and the preferred damage data combination method

Lognormal Distribution					
Drift		F(D,N)		F(γ,N)	
Lilliefors Test		Lilliefors Test		Lilliefors Test	
P	correct CDF	P	correct CDF	P	correct CDF
0.03	FALSE	0.17	TRUE	0.13	TRUE
0.17	TRUE	> 0.20	TRUE	> 0.20	TRUE
0.16	TRUE	> 0.20	TRUE	> 0.20	TRUE
0.16	TRUE	0.15	TRUE	> 0.20	TRUE
> 0.20	TRUE	> 0.20	TRUE	N.A.	N.A.

Notes: $P = P\left(D_n \le D_n^{\alpha}\right)$ where D_n^{α} is computed per Lilliefors (1967)

6.6 FRAGILITY CURVES FOR SELECTED EDPs

Figure 6.3 shows the theoretical and empirical fragility functions for use in predicting the probability that a MOR will, at least, be required given an earthquake demand on the component. Table 6.4 provides the lognormal distribution parameters defining the theoretical functions as well as the 95% confidence interval on these parameters, normalized with respect to the value of the parameter. The confidence interval (Eq. 7.1) is

$$2t\sqrt{S} \tag{7.1}$$

where t is the inverse of the student's T CDF for the 95% confidence level and S is the diagonal of the covariance matrix for the coefficient estimates. The confidence interval was computed using the MATLAB function **mle**.

Table 6.4 Lognormal distribution parameters for the three preferred EDPs

MOR	Drift				F(D,N)				F(γ,N)			
	μ		σ		μ		σ		μ		σ	
	value	95% C.I.	value	95% C.I.	value	95% C.I.	value	95% C.I.	value	95% C.I.	value	95% C.I.
0	-0.562	0.887	0.467	0.809	-1.464	0.282	0.387	0.809	-1.291	0.634	0.329	2.274
1	0.242	2.340	0.491	0.886	-1.025	0.338	0.300	0.886	-0.867	0.551	0.334	1.138
2	0.891	0.386	0.367	0.700	-0.508	0.271	0.147	0.700	-0.603	0.560	0.236	1.138
3	1.103	0.299	0.273	0.934	-0.343	0.650	0.185	0.934	-0.355	0.759	0.175	1.240
4	1.265	0.317	0.261	1.240	-0.188	0.958	0.117	1.240	N.A.	N.A.	N.A.	N.A.

Note: the 95% C.I. is the 95% confidence interval on the parameter, normalized with respect to the value of the parameter.

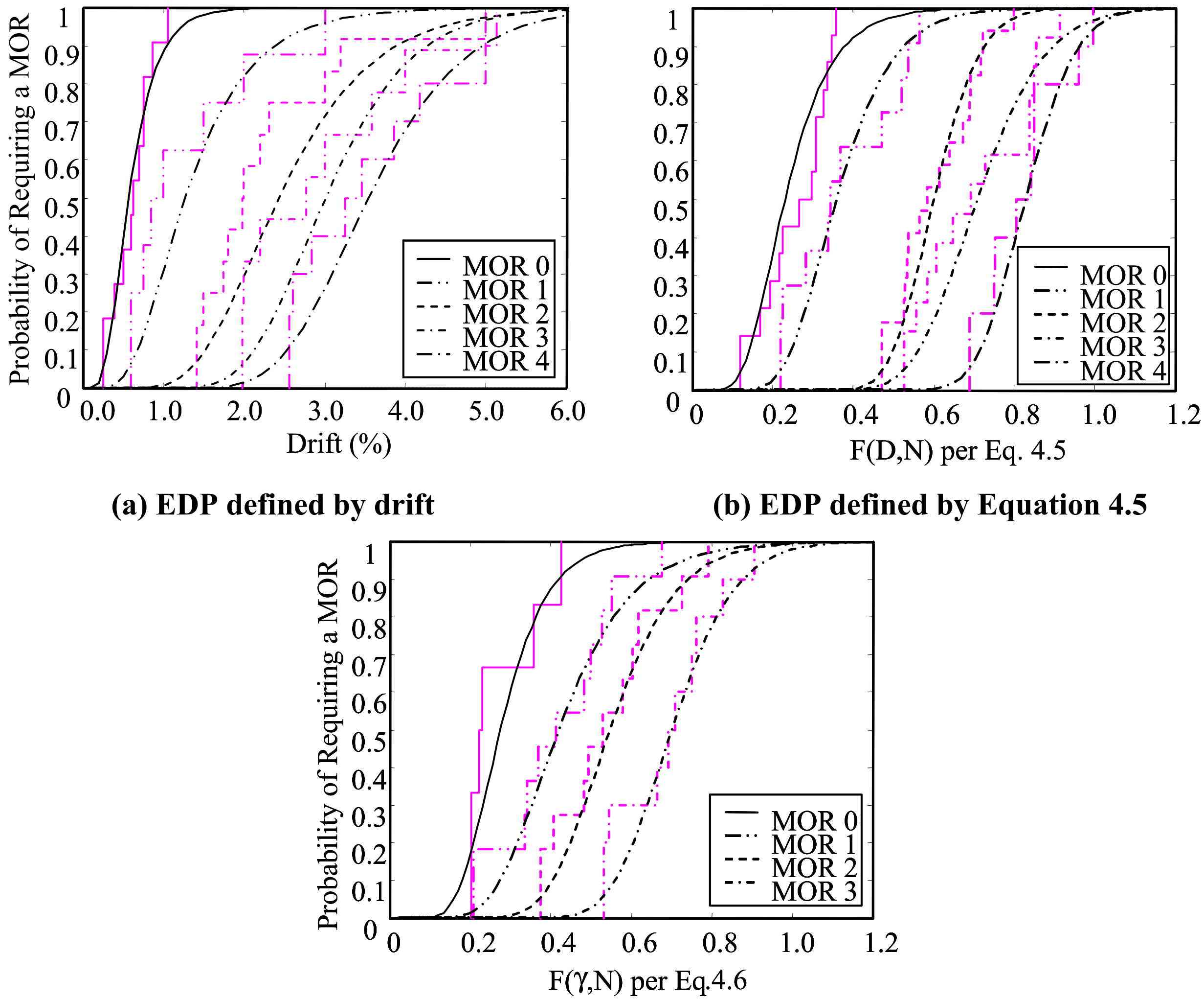

(a) EDP defined by drift

(b) EDP defined by Equation 4.5

(c) EDP defined by Equation 4.6

Figure 6.3 Theoretical (black) and empirical (grey) fragility functions

The theoretical fragility functions presented in Figure 6.3 are appropriate for use in predicting the probability that a particular MOR will be required, given an earthquake demand as defined by one of three EDPs. However, comparison of the theoretical and empirical fragility functions as well as evaluation of the confidence interval data in Table 6.4 suggests that there is significant uncertainty in the parameters that define these models. This uncertainty is due primarily to the sparsity of the data sets used to construct the models.

6.7 CONCLUSION

The probability model consists of fragility curves indicating the likelihood of requiring an MOR for a given engineering demand parameter. The fragility curves are generated for multiple data sets, distribution functions, and engineering demand parameters, and goodness-of-fit tests determine the most appropriate approach for developing the model linking an EDP to a DS and a MOR.

Three methods for grouping DSs with MOR are proposed. These methods produce three EDP-MOR data sets. All of the combination methods give approximately the same results; although Combination Method Three results in one MOR for which insufficient data are available to generate a fragility function. Thus, Combination Method Two is selected because this method balances the size of the resulting data set with the skew resulting from the introduction of higher DSs.

Three standard probability distributions are considered for modeling the empirical EDP-MOR data and thereby generating fragility curves. Evaluation of these distributions using standard goodness-of-fit tests suggests that either the lognormal or the Weibull distribution are appropriate for use in modeling the data; although it should be noted that only for the lognormal distribution is the goodness-of-fit test accurate. The lognormal distribution is chosen as the preferred distribution for use in generating the fragility functions because (1) it is a more commonly employed distribution than the Weibull distribution and (2) the goodness-of-fit test employed with the lognormal distribution is exact.

Five EDPs are considered for use in predicting joint damage. Maximum historic interstory drift, a nonlinear function of drift and number of load cycles and a nonlinear function of maximum joint shear strain demand and number of load cycles are identified as the preferred EDPs for use in predicting joint damage. These EDPs result in small coefficients of variation on the probability distribution parameters and more widely spaced means for the different MORs. Maximum joint shear strain demand was expected to be an efficient predictor of joint damage, as it defines the deformation demand imposed on the joint, while drift is a function of joint deformation as well as beam and column deformation. However, the results of this study do not suggest that joint shear strain is a particularly good indicator of damage. This may be in part because joint shear strain data were available for only half of the specimens.

7 Conclusions

The previous chapters describe the development of a model for use in predicting the method of repair required to restore an older reinforced concrete beam-column joint damaged under earthquake loading to original condition. Section 7.1 summarizes the development process. Section 7.2 identifies conclusions that can be drawn from this work. Future research needs identified as a result of this work are discussed in Section 7.3.

7.1 SUMMARY

The research presented in this report uses results from previous research to develop fragility functions that define the probability that a reinforced concrete beam-column joint subjected to earthquake loading will require a specific type of repair to restore it to pre-earthquake conditions. Previous research used to support the current investigation included experimental investigations of the earthquake response of reinforced concrete beam-column joints, investigations of the repair of reinforced concrete components including beam-column joints, and analytical studies to develop fragility functions for other structural components and systems. In Chapter 2, the results of previous research are reviewed to assemble a set of 21 experimental joint tests that characterizes the response of interior reinforced concrete beam-column joints in two-dimensional frames with design details and loads typical of pre-1967 construction on the West Coast of the United States.

The results of this study suggest that the model development process starts with identification of damage states specific to beam-column joints. In Chapter 3, the experimental tests identified in Chapter 2 are reviewed to develop a series of 13 damage states that characterize the progression of damage in beam-column joints subjected to earthquake loading. These damage states are defined by damage measures that can be observed in the laboratory and in the field: the maximum width and extent of concrete cracking, the extent of concrete spalling and crushing, and the joint failure mechanism. These damage states are defined also by damage measures that can be observed only in the laboratory: the yielding of reinforcing steel and the initiation of lateral strength loss for the joint subassemblage. The results of previous experimental investigation provide a basis for linking the proposed damage states with earthquake demand, as defined by specific engineering demand parameters. The results of previous research and construction to repair components damaged under earthquake loading provide a basis for linking these damage states with specific methods of repair.

Chapter 4 presents a series of engineering demand parameters that are appropriate for use in defining the earthquake demand imposed on a beam-column joint. The results of experimental testing of beam-column joints suggest that these demand parameters may be used to predict damage. It is expected that these demand parameters can be computed using commonly available software for nonlinear analysis of structural systems. Five engineering demand parameters are considered: maximum historic interstory drift, number of load cycles, maximum historic joint shear strain, a nonlinear function of drift and number of load cycles and a nonlinear function of shear strain and number of load cycles. Of the nonfunctional demand parameters, only for drift and number of load cycles are data provided by all experimental researchers.

Chapter 5 identifies five methods of repair that are appropriate for use in restoring earthquake damaged beam-column joints to pre-earthquake conditions. The results of previous experimental investigation of the repair of reinforced concrete components, including beam-column joints, as well as the experience of structural engineers and contractors who have accomplished post-earthquake repair provide a basis for identifying and describing these repair methods. The results of previous research and experience also provide a basis for deterministically associating a set of damage states with each of the repair methods.

Chapter 6 describes the process of developing fragility functions that define the probability that a joint subjected to a specific level of earthquake demand, as defined by a specific value of an engineering demand parameter, will require a specific method of repair to restore it to pre-earthquake conditions. The results of the 21 experimental tests identified in Chapter 2 are used to develop a series of five data sets of engineering demand parameters versus damage state data points. These data are extended to engineering demand parameters versus method of repair data using the deterministic relationships between damage and method of repair described in Chapter 5. The standard lognormal, Weibull, and beta probability distributions are calibrated using the empirical data and the method of maximum likelihood. Finally, confidence intervals on the distribution parameters and statistical goodness-of-fit tests are used to evaluate the proposed engineering demand parameters and the probability distributions. The results of this evaluation indicate that joint damage is predicted best if earthquake demand is defined by maximum historic interstory drift, a nonlinear function of drift and number of load cycles. or a nonlinear function of joint strain and number of load cycles. The results of this evaluation indicate also that the lognormal distribution may be used to model the empirical data.

7.2 CONCLUSIONS

The results of this research support several conclusions that improve understanding of the prediction of earthquake risk.

1. Five engineering demand parameters were identified as being appropriate for use in predicting earthquake-induced joint damage: maximum historic interstory drift demand, the number of load cycles, a damage index that is a nonlinear function of interstory drift and the number of load cycles, maximum historic joint shear strain demand, and a damage index that is a nonlinear function of joint shear strain and number of load cycles. Of these parameters, drift and the functional damage indexes are the best indicators of joint damage.
2. Earthquake-induced damage sustained by beam-column joints may be described using a series of 13 damage states. These damage states characterize damage primarily on the basis of the extent and magnitude of concrete cracking, the extent of concrete crushing and spalling and failure. These damage states can be associated with specific methods of repair.
3. Three standard probability distributions (lognormal, Weibull, and beta) were considered to fit the empirical engineering demand parameter versus required method of repair data. Applying standard statistical goodness-of-fit tests to evaluate these distributions indicates that lognormal is the best distribution for use in modeling the empirical data.

7.3 FUTURE RESEARCH NEEDS

This report describes the initial development of a model that can be used to predict the method of repair required to restore a beam-column joint damaged under earthquake loading. The model development process includes several steps, and at each step in the process, there is an opportunity to include additional information that will improve the model and reduce the uncertainty in the predicted impact of the earthquake damage. The following paragraphs suggest ways in which the model may be improved.

Fragility functions indicating the probability that a joint subjected to earthquake loading will require a method of repair can be improved by adding additional experimental data. First, the computed confidence intervals on the fragility function parameter indicate that the fragility curves are highly uncertain. This uncertainty is directly attributable to the small size of the data sets used to generate the functions. More experimental data characterizing the progression of damage observed under earthquake loading will reduce the uncertainty inherent in the fragility functions. Second, the results of the current study suggest that earthquake demand is defined best by maximum interstory drift, a nonlinear function of maximum interstory drift and number of load cycles, or a nonlinear function of joint shear strain and number of load cycles. The results of this study do not indicate that maximum joint shear strain is a particularly good indicator of damage. However, joint shear strain could be expected to be a particularly good predictor of joint damage, since, unlike drift, it includes only the deformation demand imposed on the joint. These results may be because relatively few researchers provide joint shear strain data, and thus the joint strain data set is particularly small. Thus, additional experimental testing to generate joint shear strain and damage data is required to improve joint fragility functions using joint shear strain as a demand parameter.

Application of the predictive models developed as part of this project requires the output of a nonlinear structural analysis. The analysis output is the engineering demand parameter from which the required method of repair is predicted using the proposed fragility functions. Inherent in this process is the assumption that the nonlinear response of the structure is predicted accurately, including nonlinear joint shear strain. Thus, accurate models are required for use in predicting the nonlinear response of structural systems, including joint response.

The results of this study include fragility functions that predict the method of repair required to restore a joint to pre-earthquake conditions. However, for a building owner, the economic impact of an earthquake is measured in terms of the total cost required to restore the entire structure and its contents to pre-earthquake conditions and the time required to accomplish this. Thus, additional research is required to generate cost and downtime information for repair of beam-column joints as well as to develop a comprehensive framework for computing cost and downtime for global structural repair.

References

Alire, D. (2002). "Seismic Evaluation of Existing Unconfined Reinforced Concrete Beam-Column Joints." *M.S. Thesis*. Seattle: University of Washington.

American Concrete Institute (1968). *Epoxies with Concrete*, *ACI SP-21*.

American Concrete Institute (2002). "Building Code Requirement for Reinforced Concrete." *ACI 318-95*.

American Concrete Institute (1996). *Concrete Repair Guide ACI 546R-96*.

Bonacci, J.F. and J. Wight (1996). "Displacement-Based Assessment of Reinforced Concrete Frames in Earthquakes." *ACI SP 162*: 117-138.

Bonacci, J.F., and S. Pantazopoulou (1993). "Parametric Investigation of Joint Mechanisms." *ACI Structural Journal* 90 (1): 61-71.

Coffman, H. and J. Kapur (March 2003). Washington Department of Transportation. In-person interview.

David, F.N. and N.L. Johnson (1948). "The Probability Integral Transformation When Parameters Are Estimated from the Sample." *Biometrika* (35):182-190.

Durrani, A. and J. Wight (1982). "Experimental and Analytical Study of Internal Beam to Column Connections Subjected to Reversed Cyclic Loading." *Report UMEE 82R3*.

Federal Emergency Management Agency (1997). *NEHRP Guidelines for the Seismic Rehabilitation of Buildings FEMA-273*.

Federal Emergency Management Agency (1998). *Repair of Earthquake Damaged Concrete and Masonry Wall Buildings FEMA 308*.

Filiatrault, A. and I. Lebrun (1996). "Seismic Rehabilitation of Reinforced Concrete Joints by Epoxy Pressure Injection Technique." *ACI SP 160*: 73-92.

French, C. W., G.A. Thorp and W.J. Tasai (1990). "Epoxy Repair Techniques for Moderate Earthquake Damage." *ACI Structural Journal* 87 (4): 416-424.

Hakuto, S., R. Park and H. Tanaka (1997). “Seismic Load Tests on Interior and Exterior Beam-Column Joints with Substandard Reinforcing Details.” *ACI Structural Journal* 97 (1): 11-25.

Haldar, A. and S. Mahadevan (2000). *Probability, Reliability, and Statistical Methods for Engineering Design*. New York: John Wiley and Sons, Inc.

Hanson, N.W. and H.W. Conner (1967). “Seismic Resistance of Reinforced Concrete Beam-Column Joints.” *Journal of the Structural Division, ASCE* 93 (ST5): 533-560.

Hoel, P.G. (1962). *Introduction to Mathematical Statistics*, 3rd Ed. New York: John Wiley and Sons, Inc.

Jara, M., G. Hernandez and Robles (1989). “The Mexico Earthquake of September 19, 1985-Typical Cases of Repair and Strengthening of Concrete Buildings.” *Earthquake Spectra* 5 (1): 175-181.

Joh, Goto and Shibata (1991). “Influence of Transverse Joint and Beam Reinforcement and Relocation of Plastic Hinge Region on Beam-Column Joint Stiffness Deterioration.” *ACI SP-123*. No. 8.

Joh, Goto, and Shibata (1991). “Behavior of Reinforced Concrete Beam-Column Joints with Eccentricity.” *ACI SP-123*. No. 12.

Kamimura, T., S. Takeda and M. Tochio (2000). “Influence of Joint Reinforcement on Strength and Deformation of Interior Beam-Column Subassemblages.” *Proceedings of the 12th World Conference on Earthquake Engineering.* Auckland, New Zealand. No. 2267.

Karayannis, C.G., C.E. Chalioris and K.K. Sideris (1998). “Effectiveness of RC Beam-Column Connection Repair using Epoxy Resin Injections.” *Journal of Earthquake Engineering* 2 (2): 217-240.

Kitayama, K., S. Otani and H. Aoyama (1991). “Development of Design Criteria for RC Interior Beam-Column Joints.” *ACI SP-123*: 96-123.

Kottegoda, N.T. and R. Rosso (1997). *Probability, Statistics and Reliability for Civil and Environmental Engineers*. Boston: McGraw-Hill Custom Publishing. 735 pp.

Leon, R.T. (1990). “Shear Strength and Hysteretic Behavior of Interior Beam-Column Joints.” *ACI Structural Journal* **87** (1): 3-11.

Lowes, L.N. (1999). “Finite Element Modeling of Reinforced Concrete Beam-Column Bridge Connections.” *Diss.* Berkeley: *University of California*.

Lilliefors, H.W. (1967). "On the K-S Test for Normality with Mean and Variance Unknown." *Journal of the American Statistical Association* 62: 399-402.

MATLAB (2000). Natick, Mass.: The MathWorks.

Mitchell, DeVall, Kobayashi, Tinawi and Tso (1996). "Damage to Concrete Structures due to the January 17, 1995 Hyogo-ken Nanbu (Kobe) Earthquake." *Canadian Journal of Civil Engineering* 23: 757-777.

Meinheit, D. and J. Jirsa (1977). "The Shear Strength of Reinforced Concrete Beam-Column Joints." *CESRL Report*. Austin: University of Texas.

Meinheit, D. and J. Jirsa (1981). "Shear Strength of R/C Beam-Column Connections." *Journal of the Structural Division* 107 (ST11): 2227-2243.

Miller, L.H. (1956). "Table of Percentage Points of Kolmogorov Statistics." *Journal of the American Statistical Association* 51: 111-121.

Mosier, W.G. (2000). "Seismic Assessment of Reinforced Concrete Beam-Column Joints." *M.S.*

Nakashima, M., K. Ogawa, and K. Inque (2001). "Generic Frame Model for Simulation for Earthquake Responses of Steel Moment Frames." *Earthquake Engineering and Structural Dynamics* 31:671-692.

Newman, A. (2001). *Structural Renovation of Buildings.* New York: McGraw-Hill.

Park, R. and D. Ruitong (1988). "A Comparison of the Behavior of Reinforced Concrete Beam-Column Joints Designed for Ductility and Limited Ductility." *Bulletin of the New-Zealand National Society for Earthquake Engineering* 21 (4): 255-278.

Pessiki, S.P., C. Conley, P. Gergely and R.N. White (1990). "Seismic Behavior of Lightly-RC Column and Beam-Column Joint Details." *NCEER-90-0014*. Buffalo: National Center for Earthquake Engineering.

Pessiki, S.P., C. Conley, R.N. White and P. Gergely (1990). "Seismic Behavior of the Beam-Column Connection Region in Lightly-Reinforced Concrete Frame Structures." *Proceedings of Fourth National Conference on Earthquake Engineering May 20-24, Palm Springs California*. Oakland: EERI. 707-716.

Porter, Beck, and Shaikhutdinov (2002). "Sensitivity of Building Loss Estimates to Major Uncertain Variables." *Earthquake Spectra* 18.

Portland Cement Association (1967). *Preliminary Report: The Behavior of Reinforced Concrete Structures in the Caracas, Venezuela Earthquake of July 29, 1967*." 34 pp.

Raynor, D.J., D.E. Lehman D.E. and J.F. Stanton (2002). “Bond-slip response of reinforcing bars grouted in ducts.” *ACI Structural Journal* 99 (5): 568-576.

Runacres, R. (February 2003). Contech, Inc. Telephone interview.

Rutherford & Chekene, Consulting Engineers (1992). *Seismic Upgrading Study of the Main Public Library Building San Francisco, CA for the Asian Art Museum at the Civic Center: Study Report volume 1:* C.9-C.43.

Savage, S. (March 2003). Coughlin, Porter, and Lundeen. In-person interview.

Saxena, Deodatis, Shinozuka, and Feng (2000). “Development of Fragility Curves for Multi-Span Reinforced Concrete Bridges.” *MCEER Report*. Buffalo: Multidisciplinary Center for Earthquake Engineering Research.

Shima, H., L.L. Chou and H. Okamura (1987). “Bond Characteristics in Post-Yield Range of Deformed Bars.” *Concrete Library of JSCE* **10**: 113-124.

Shinozuka, Masanobu, Feng, Lee, and Naganuma (2000). “Statistical Analysis of Fragility Curves.” *Journal of Engineering Mechanics*.

Shiohara, H. (1999). “Lifecycle Economic Loss Estimation of R/C frame Structure Subjected to Multiple Earthquake Load Sequences.” *US-Japan Workshop of Performance-Based Earthquake Engineering Methodology for Reinforced Concrete Building Structures, PEER Report 10/99*:161-173.

Tasai, A. (1992) “Effective Repair with Resin for Bond Failure of RC Members.” *Proceedings of the 10th World Conference on Earthquake Engineering:* 5211-5216.

Uzmeri, S.M. (1978). “Strength and Ductility of Cast-In-Place Beam-Column Joints.” *ACI SP-53*. No. 12.

Walker, S. (2001). “Seismic Performance of Existing Reinforced Concrete Beam-Column Joints.” *M.S. Thesis*. Seattle: University of Washington..

Zaid, Safaa, Otani, and Shiohara (2001). “Behavior of Reinforced Concrete Beam-Column Connections under EQ Loading.” *Thesis*. Tokyo: University of Tokyo.

Zhang, L. and J. Jirsa (1982). “A Study of Shear Behavior of Reinforced Concrete Beam-Column Joints.” *PMSFEL Report 82-1*. Austin: University of Texas.

Appendix A: Questions and Answers from Personal Interviews

A.1 QUESTIONS PRESENTED TO INDUSTRY PROFESSIONALS

A.1.1 Slides Presented to Interviewees

Research Objective: Predict Earthquake Loss

The results of structural analysis defines the earthquake demand on structural component. Component specific fragility curves have been developed to predict the damage state of reinforced concrete components given demand.

Now, we must predict the earthquake loss.

Earthquake loss is determined by the cost of restoring the structural components to their original condition and structural downtime associated with repair.

Objectives for Today's Discussion :

1- *Confirm* the repair techniques are accurately described, most commonly used, and are effective at restoring components to original capacity.

2- *Link* the correct repair techniques with each of the damage levels.

3- *Define* the economic loss associated with the repair techniques. Loss is a function of the total cost and the total repair time.

Repair Technique:

#0- Cosmetic repair of nonstructural materials.

Description:
Repair nonstructural material covering structural components.

NOTE:
All subsequent repair techniques are assumed to require repair and/or removal and replacement of architectural finish. These costs will need to be included in estimating earthquake loss.

Repair Techniques:

#1a- Epoxy resin injection of cracked concrete.

***Description*:**
Cracked concrete is appropriate for pressure injection when crack widths exceed 0.002in.

0.75 in. is the maximum crack width that is appropriate for epoxy resin injection. Shear cracks are not appropriate for epoxy injection if crack width exceeds 0.04 in. (Filiatrault, SP160-3)

#1b- Epoxy and aggregate repair of cracked concrete.
***Description*:**
Larger cracks require a gap-graded aggregate to be added to the epoxy adhesive.
The aggregate is placed in the crack, and a low or medium viscosity epoxy is injected.

Repair Techniques:

#1a - Epoxy resin injection of cracked concrete.
#1b - epoxy injection + aggregate

Description:

- epoxy inject cracks
  - crack widths may range from 0.002 in. to 0.75 in.
  - practical minimum crack widths for injection 1/32 in. to 1/16 in.
- epoxy injection with aggregate / low-pressure cementitious material
  - if crack width exceeds 0.75 in. graded aggregate may be introduced into the crack or cementitious material used.

Repair Technique:

#2- Cement or epoxy mortar paste is used to replace spalled concrete.

Description:
Spalling of the concrete must be limited to a width and depth where the reinforcement is not exposed.

Here it is assumed that the depth of spalled concrete is less than 6″; thus an epoxy adhesive must be used to bond the new material to the original concrete.

If cracks surround the spalled area, repair #1 is also required.

Repair Technique:

#3- Damaged concrete is removed and replaced with concrete, cement paste or epoxy mortar paste

Description of damage:

- Spalled concrete exposes reinforcement.
- Confined concrete is crushed and/or severely cracked.

Repair:

- remove damaged concrete as is necessary (chipping / jack hammering used)
- replace concrete with new concrete, cement paste, mortar
- jacketing may be appropriate

Note

- This repair will likely require the removal of nonstructural elements in the vicinity of the structural component.

Repair Technique:

#4-Removal and replacement of exposed and damaged rebar. Correction of residual deformations when necessary.

Description:
Spalling of the concrete exposes the reinforcement. Confined concrete is crushed and little or no bond exists between the concrete and the steel.

Removal of the damaged reinforcement and crushed concrete is required. Additional concrete may be removed.

Note:
This repair will likely require the removal of nonstructural elements in the vicinity of the structural component.

Damage Level 1: Joint

Description:
Initial cracks at beam-column interface.
Initial diagonal cracks within joint area.

Repair:
#0
or
#1a

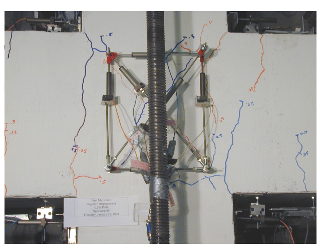

Damage Level 1: Joint

Description:
Beam longitudinal reinforcement yields.

Diagonal crack widths grow from hairline to 0.02″ to 0.09″.

Repair:
#1a
or
#1b

Damage Level 2: Joint

Description:
Initial spalling of joint-region concrete (<30% of area).
Onset of joint shear resistance deterioration.

Repair
#2

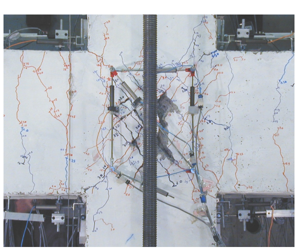

Damage Level 2: Joint

Description:
More than 30% of joint area concrete has spalled.

Cracks extend into beam and/or column.

Repair:
#2

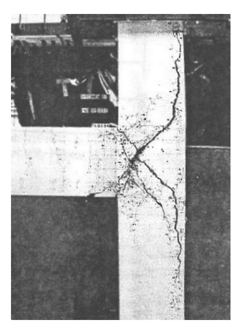

Damage Level 3: Joint

Description:
More than 80% of joint area concrete has spalled.

Crushing of concrete extends into joint depth.

Corner column rebar is exposed.

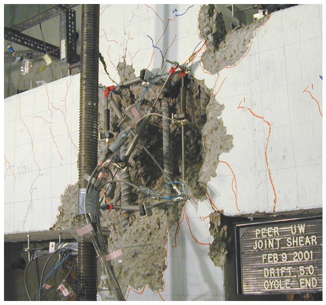

Damage Level 3: Joint

Description:
Catastrophic failure defined by buckling of column rebar,
Or beam pulls away from joint,
Or embedded rebar pulls out of joint.

Repair:
#3

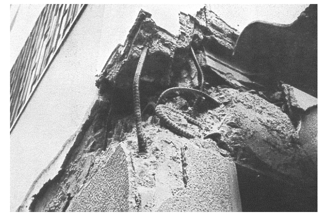

Column:
Ductile Behavior

Damage Level 1
Description:
Flexural (horizontal) cracks.
Flexural crack width ≤ 0.75″.
Repair:#1a

Damage Level 2
Description:
Onset of spalling.
Spalling height ≥10% d_c
Repair: #2

Damage Level 3
Description:
Initiation of bar buckling.
Fracture of transverse steel.
Fracture of longitudinal steel.
Repair:#3

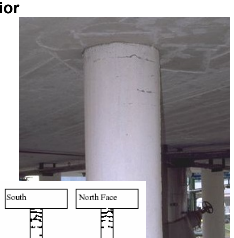

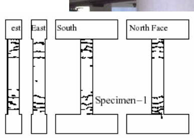

Column
Brittle Behavior

Damage Level 1
Description:
Diagonal cracks extend over 25% d_c
Vertical cracks extend over 10% d_c
Crack width ≤ 0.04″.
Repair:#1a

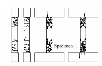

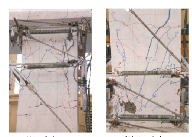

Damage Level 2 and 3
Description:
Diagonal cracks extend over 67% d_c
Vertical cracks extend over 67% d_c
Crack width > 0.08″.
Repair: Previously undefined

Defining Loss for Repair #0:
No picture available.

Unit cost of
-Material: Must match aesthetic properties of the existing material.

-Equipment: Removal tools, such as hammers and grinders, and mixing and placing tools are needed.

-Personnel: Experienced personnel with the material manufacturer certification when appropriate.

Total Repair Time:
Estimated time of mobilization, demolition, and replacing architectural finish plus the amount of time required for setting of new material.

Defining Loss for Repair #1a & b:
Refer to pictures.

Unit cost of
-Material: Low viscosity injectable epoxy adhesive. Gap-grade aggregate for large cracks. Medium viscosity injectable epoxy adhesive.

-Equipment: Pressure injection machine. Ports, drills, and sealant. Mixing and pressure monitoring equipment.

-Personnel: Experienced personnel with material testing skills.

Total Repair Time:
Estimated time of surface preparation, adhesive injection, and surface finishing plus the amount of time required for setting of new material.

Defining Loss for Repair #2:
Refer to pictures.

Unit cost of
-Material: Cement or epoxy mortar paste

-Equipment: Hammers, grinders, and concrete saws. Mixing and placing tools.

-Personnel: Experienced personnel with the material manufacturer certification when appropriate.

Total Repair Time:
Estimated time of concrete removal, paste application, and surface finishing plus the amount of time required for setting of new material.

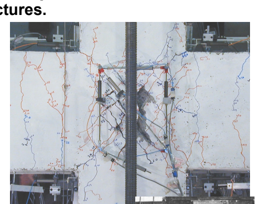

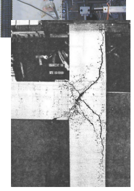

Defining Loss for Repair #3:
Refer to pictures.

Unit cost of
-Material: Rebar and mechanical connection device.

-Equipment: Power tools and hydraulic press if needed.

-Personnel: Experienced personnel with consultation of device manufacturer when appropriate.

Total Repair Time:
Estimated time of rebar removal and placing and securing new rebar.

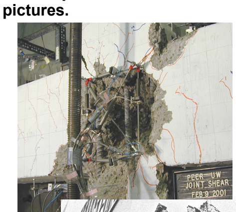

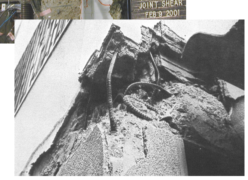

Defining Loss for Repairing Residual Deformations Associated with Damage Levels 2 and 3:

Unit cost of

-Material: **No additional materials required.**

-Equipment: **Crane or other large machinery.**

-Personnel: **Experienced personnel.**

Total Repair Time:
Estimated time of achieving original alignment of component plus time acquiring engineer's assessment.

A.1.2 Questions Regarding Proposed Repair Techniques

1. Are there additional repair techniques that should be considered?
2. Residual deformation has been associated with repair techniques #2 and #3 when higher levels of damage are anticipated. At what drift level would the residual deformation be (a) ignored, (b) corrected, and (c) cause the building to be replaced?
3. How significantly do the environmental conditions affect material selection for a RC component in a building where cladding and other nonstructural elements provide protection?
4. Are these repair techniques appropriate for beam-column joints as well as columns?
5. Are there subdivisions within the repair techniques listed above that are associated with substantially different costs?
6. A variety of application processes accompany these repair techniques, e.g., vacuum versus high-pressure injection. Why would a more expensive process be selected?

A.1.3 Questions Regarding Linking Repair Technique to Damage in Joints

1. What damage measures would trigger use of Repair Technique #1 — epoxy injection?
2. What damage measures would trigger use of Repair Technique #2 — patching? Diagonal or vertical cracks ≥ 0.04″ or 0.75″? Onset of spalling?
3. What damage measures would trigger use of Repair Technique #3 — replacement of joint? Onset of significant spalling? Loss of bond strength within the joint? First sign of buckling of reinforcing steel?
4. What damage measure would result in an unrepairable joint? Significant buckling of longitudinal reinforcing steel? Fracture of transverse reinforcing steel? Fracture of longitudinal reinforcing steel? Fracture of multiple longitudinal reinforcing bars?

A.1.4 Questions Regarding Linking Repair Techniques to Damage in Columns

For the column considered to exhibit a flexural response mechanism:

1. What damage measures would trigger use of Repair Technique #1 — epoxy injection? Horizontal (flexural) cracks ≥ 0.75″? Horizontal (flexural) cracks distributed over a height extending 50% of the column cross-section depth?
2. What damage measures would trigger use of Repair Technique #2 — patching? Horizontal (flexural) cracks ≥ 2 mm? Horizontal (flexural) cracks distributed over a height extending 50% of the column height? Onset of spalling? Onset of significant spalling?
3. What damage measures would trigger use of Repair Technique #3 — replacement of column? First sign of buckling of reinforcing steel? Significant buckling of longitudinal reinforcing steel?
4. What damage measures would result in an unrepairable column? Fracture of transverse reinforcing steel? Fracture of longitudinal reinforcing steel? Fracture of multiple longitudinal reinforcing bars?

For the column considered to exhibit a brittle (shear or bond-failure) response mechanism:

1. What damage measures would trigger use of Repair Technique #1 — epoxy injection? Visible diagonal cracking? Sources indicate that shear cracks >0.04″ can not be repaired using epoxy injection. Is this true for vertical cracks as well?
2. What damage measures would result in an unrepairable column? What is the appropriate repair for the onset of the shear or bond-failure mechanisms? Shear mechanism is defined by diagonal cracking over 67% of the column depth and crack width > 0.08″. Bond-failure is cracks extending vertically over 67% of column depth and crack width > 0.08″.

A.1.5 Defining Loss Due to Repair

1. Loss has been defined as the unit cost of material, unit cost of equipment, and the unit cost of personnel plus the amount of downtime in terms of days. Is this the same definition loss used for estimation in practice?
2. Is it possible to set up rules to estimate the start-up cost of the repair technique. Start-up cost would include mobilization and demolition to the extent required for the level of damage. For example, how can I estimate the start-up cost associated with epoxy injection of 10 columns versus 100 columns?
3. Is it possible to estimate the cost of the architectural finish?
4. What is the per-unit material cost associated with the repair technique? Will this vary substantially if the concrete crack widths are 0.05″ versus 0.2″? Or if the height of spalling on a concrete column is 12″ versus 24″?
5. How long will it take to accomplish repair of a single unit and what would be the labor rate? Will repair time vary substantially if there are 10 units versus 100 units?

6. Can the building be occupied while repair is accomplished?

A.2 INTERVIEW WITH S. SAVAGE

A.2.1 Contact Information

Steve J. Savage, P.E.
Associate, Coughlin, Porter, and Lundeen
217 Pine Street
Suite 300
Seattle, WA 98101
Phone: 206-334-0460
Fax:
E-Mail: steves@cplinc.com

A.2.2 Comments Regarding Questions:

Question 1: Repair methods are complete.

Question 2: For steel, correction of residual deformation depends on type of system. For concrete, correction of residual deformation is not possible. The offset may be within the limits of the building code and could be ignored.

Question 4: Repair methods for columns in addition to those provided are wrapping, i.e., jacketing. A combination of epoxy injection and jacketing would be most applicable in damage seen in the figure (Hakuto ext.)

Question 7: When determining the "trigger" damage state for a repair method, analysis of capacity is best. If not possible, then repair will be recommended.

Question 11: Determining "trigger" for repair of flexural response of column requires analysis, if available, to determine amount of inelastic response already used. Flexural cracks will require less amount of repair. Epoxy resin injection: Lower bound crack width is 1/16″. New concrete: Remove damaged joint core by jack-hammering.

Question 12: Patching of damaged concrete can be used until crushing of concrete occurs. No jacketing of flexural response should be required.

Questions 13 and 14: Enlargement due to concrete crushing repaired with jacket. Must be observant of stiffness changes and shear force capacity after repair for future analysis. Cost effiency: Jacketing is best if several columns are to be repaired. Replacement is best if only one column is damaged.

Question 15: The "trigger" for replacement or jacketing of brittle response of column is when the cracks get into middle third of column. Cracks just at end (seen in figure (Sezen)) would require replacing or jacketing. Cost increases: Replacement of column requires shoring. This increases the cost beyond that expected for jacketing.

Question 17: Cost of repair is determined by contractors.

Question 18: Developing rules for start-up cost would involve establishing a /ft^2 cost based on quantity of components. Must specify the following for estimate from general contractor: close environment (office) versus open environment, vintage, quality, type of use, partitioning material will drive cost.

A.3 INTERVIEW WITH H. COFFMAN AND J. KAPUR:

A.3.1 Contact Information

Harvey Coffman
Bridge Preservation Engineer
WSDOT
Phone: 360-570-2556
E-Mail: coffmah@wsdot.wa.gov

J Kapur
Bridge Design Engineer
WSDOT
Phone: 360-705-7209
E-Mail: kapurju@wsdot.wa.gov

A.3.2 Comments Regarding Cost:

1. Contributing factors to cost
    a. Lack of contractors
    b. Lack of labor
    c. Lack of equipment
2. Traffic control
    a. High tolerance— allow work to be done during day
    b. Low tolerance— require work to be done at night at time and a half

A.3.3 Comments Regarding Repair

1. Epoxy resin injection
    a. Use when crack width is >1mm (0.025″).
    b. Potential corrosion of rebar
    c. May use if smaller crack lends to reduced capacity.
    d. Lineal ft. of cracks to determine amt./ cost of adhesive
    e. **Cost is $10/ft**.
2. Spalling
    a. Paint rebar with epoxy to prevent corrosion.
    b. Place chicken wire after spalled concrete is removed.
3. Steel jacketing
    a. Square column may be repaired with circular can and filled with grout.
    b. Cost is $1000/ft.
4. Damage specific to bridge
    a. Little experience with damage caused by EQ in Washington; however may be comparable to damage due to scour
    b. Concentrated in superstructure
    c. Shoring is done immediately to prevent additional damage and continue use of bridge.
    d. Monitoring of cracks with crack gauges to decide if repair is necessary.

e. Restoring residual deformation can be done using jacks and rollers.
f. Column
    i. cracking at cover indicates cracking through width.
    ii. chip off cover concrete if
        1. core into core to test for internal damage
        2. hammer test yields spalling
    iii. crushing and cracking of core
        1. remove substantial amt. of concrete
        2. replace concrete

5. Note that our repair method #3 is considered repair level #1 for WSDOT. Prior to that, the damage is not severe enough.

PEER REPORTS

PEER reports are available from the National Information Service for Earthquake Engineering (NISEE). To order PEER reports, please contact the Pacific Earthquake Engineering Research Center, 1301 South 46th Street, Richmond, California 94804-4698. Tel.: (510) 231-9468; Fax: (510) 231-9461.

PEER 2004/05 *Performance-Based Seismic Design Concepts and Implementation: Proceedings of an International Workshop.* Peter Fajfar and Helmut Krawinkler, editors. September 2004.

PEER 2004/02 *Analytical Investigations of New Methods for Reducing Residual Displacements of Reinforced Concrete Bridge Columns.* Junichi Sakai and Stephen A. Mahin. August 2004.

PEER 2004/01 *Seismic Performance of Masonry Buildings and Design Implications.* Kerri Anne Taeko Tokoro, James C. Anderson, and Vitelmo V. Bertero. February 2004.

PEER 2003/18 *Performance Models for Flexural Damage in Reinforced Concrete Columns.* Michael Berry and Marc Eberhard. August 2003.

PEER 2003/17 *Predicting Earthquake Damage in Older Reinforced Concrete Beam-Column Joints.* Catherine Pagni and Laura Lowes. October 2004.

PEER 2003/16 *Seismic Demands for Performance-Based Design of Bridges.* Kevin Mackie and Božidar Stojadinović. August 2003.

PEER 2003/15 *Seismic Demands for Nondeteriorating Frame Structures and Their Dependence on Ground Motions.* Ricardo Antonio Medina and Helmut Krawinkler. May 2004.

PEER 2003/14 *Finite Element Reliability and Sensitivity Methods for Performance-Based Earthquake Engineering.* Terje Haukaas and Armen Der Kiureghian. April 2004.

PEER 2003/13 *Effects of Connection Hysteretic Degradation on the Seismic Behavior of Steel Moment-Resisting Frames.* Janise E. Rodgers and Stephen A. Mahin. March 2004.

PEER 2003/12 *Implementation Manual for the Seismic Protection of Laboratory Contents: Format and Case Studies.* William T. Holmes and Mary C. Comerio. October 2003.

PEER 2003/11 *Fifth U.S.-Japan Workshop on Performance-Based Earthquake Engineering Methodology for Reinforced Concrete Building Structures.* February 2004.

PEER 2003/10 *A Beam-Column Joint Model for Simulating the Earthquake Response of Reinforced Concrete Frames.* Laura N. Lowes, Nilanjan Mitra, and Arash Altoontash. February 2004.

PEER 2003/09 *Sequencing Repairs after an Earthquake: An Economic Approach.* Marco Casari and Simon J. Wilkie. April 2004.

PEER 2003/08 *A Technical Framework for Probability-Based Demand and Capacity Factor Design (DCFD) Seismic Formats*. Fatemeh Jalayer and C. Allin Cornell. November 2003.

PEER 2003/07 *Uncertainty Specification and Propagation for Loss Estimation Using FOSM Methods.* Jack W. Baker and C. Allin Cornell. September 2003.

PEER 2003/06 *Performance of Circular Reinforced Concrete Bridge Columns under Bidirectional Earthquake Loading*. Mahmoud M. Hachem, Stephen A. Mahin, and Jack P. Moehle. February 2003.

PEER 2003/05 *Response Assessment for Building-Specific Loss Estimation.* Eduardo Miranda and Shahram Taghavi. September 2003.

PEER 2003/04 *Experimental Assessment of Columns with Short Lap Splices Subjected to Cyclic Loads*. Murat Melek, John W. Wallace, and Joel Conte. April 2003.

PEER 2003/03 *Probabilistic Response Assessment for Building-Specific Loss Estimation.* Eduardo Miranda and Hesameddin Aslani. September 2003.

PEER 2003/02 *Software Framework for Collaborative Development of Nonlinear Dynamic Analysis Program.* Jun Peng and Kincho H. Law. September 2003.

PEER 2003/01 *Shake Table Tests and Analytical Studies on the Gravity Load Collapse of Reinforced Concrete Frames.* Kenneth John Elwood and Jack P. Moehle. November 2003.

PEER 2002/24 *Performance of Beam to Column Bridge Joints Subjected to a Large Velocity Pulse.* Natalie Gibson, André Filiatrault, and Scott A. Ashford. April 2002.

PEER 2002/23 *Effects of Large Velocity Pulses on Reinforced Concrete Bridge Columns.* Greg L. Orozco and Scott A. Ashford. April 2002.

PEER 2002/22 *Characterization of Large Velocity Pulses for Laboratory Testing.* Kenneth E. Cox and Scott A. Ashford. April 2002.

PEER 2002/21 *Fourth U.S.-Japan Workshop on Performance-Based Earthquake Engineering Methodology for Reinforced Concrete Building Structures*. December 2002.

PEER 2002/20 *Barriers to Adoption and Implementation of PBEE Innovations.* Peter J. May. August 2002.

PEER 2002/19 *Economic-Engineered Integrated Models for Earthquakes: Socioeconomic Impacts.* Peter Gordon, James E. Moore II, and Harry W. Richardson. July 2002.

PEER 2002/18 *Assessment of Reinforced Concrete Building Exterior Joints with Substandard Details.* Chris P. Pantelides, Jon Hansen, Justin Nadauld, and Lawrence D. Reaveley. May 2002.

PEER 2002/17 *Structural Characterization and Seismic Response Analysis of a Highway Overcrossing Equipped with Elastomeric Bearings and Fluid Dampers: A Case Study.* Nicos Makris and Jian Zhang. November 2002.

PEER 2002/16 *Estimation of Uncertainty in Geotechnical Properties for Performance-Based Earthquake Engineering.* Allen L. Jones, Steven L. Kramer, and Pedro Arduino. December 2002.

PEER 2002/15 *Seismic Behavior of Bridge Columns Subjected to Various Loading Patterns.* Asadollah Esmaeily-Gh. and Yan Xiao. December 2002.

PEER 2002/14 *Inelastic Seismic Response of Extended Pile Shaft Supported Bridge Structures.* T.C. Hutchinson, R.W. Boulanger, Y.H. Chai, and I.M. Idriss. December 2002.

PEER 2002/13 *Probabilistic Models and Fragility Estimates for Bridge Components and Systems.* Paolo Gardoni, Armen Der Kiureghian, and Khalid M. Mosalam. June 2002.

PEER 2002/12 *Effects of Fault Dip and Slip Rake on Near-Source Ground Motions: Why Chi-Chi Was a Relatively Mild M7.6 Earthquake.* Brad T. Aagaard, John F. Hall, and Thomas H. Heaton. December 2002.

PEER 2002/11 *Analytical and Experimental Study of Fiber-Reinforced Strip Isolators*. James M. Kelly and Shakhzod M. Takhirov. September 2002.

PEER 2002/10 *Centrifuge Modeling of Settlement and Lateral Spreading with Comparisons to Numerical Analyses***.** Sivapalan Gajan and Bruce L. Kutter. January 2003.

PEER 2002/09 *Documentation and Analysis of Field Case Histories of Seismic Compression during the 1994 Northridge, California, Earthquake.* Jonathan P. Stewart, Patrick M. Smith, Daniel H. Whang, and Jonathan D. Bray. October 2002.

PEER 2002/08 *Component Testing, Stability Analysis and Characterization of Buckling-Restrained Unbonded Braces™.* Cameron Black, Nicos Makris, and Ian Aiken. September 2002.

PEER 2002/07 *Seismic Performance of Pile-Wharf Connections.* Charles W. Roeder, Robert Graff, Jennifer Soderstrom, and Jun Han Yoo. December 2001.

PEER 2002/06 *The Use of Benefit-Cost Analysis for Evaluation of Performance-Based Earthquake Engineering Decisions*. Richard O. Zerbe and Anthony Falit-Baiamonte. September 2001.

PEER 2002/05 *Guidelines, Specifications, and Seismic Performance Characterization of Nonstructural Building Components and Equipment*. André Filiatrault, Constantin Christopoulos, and Christopher Stearns. September 2001.

PEER 2002/04 *Consortium of Organizations for Strong-Motion Observation Systems and the Pacific Earthquake Engineering Research Center Lifelines Program: Invited Workshop on Archiving and Web Dissemination of Geotechnical Data, 4–5 October 2001*. September 2002.

PEER 2002/03 *Investigation of Sensitivity of Building Loss Estimates to Major Uncertain Variables for the Van Nuys Testbed.* Keith A. Porter, James L. Beck, and Rustem V. Shaikhutdinov. August 2002.

PEER 2002/02 *The Third U.S.-Japan Workshop on Performance-Based Earthquake Engineering Methodology for Reinforced Concrete Building Structures*. July 2002.

PEER 2002/01 *Nonstructural Loss Estimation: The UC Berkeley Case Study.* Mary C. Comerio and John C. Stallmeyer. December 2001.

PEER 2001/16 *Statistics of SDF-System Estimate of Roof Displacement for Pushover Analysis of Buildings.* Anil K. Chopra, Rakesh K. Goel, and Chatpan Chintanapakdee. December 2001.

PEER 2001/15 *Damage to Bridges during the 2001 Nisqually Earthquake.* R. Tyler Ranf, Marc O. Eberhard, and Michael P. Berry. November 2001.

PEER 2001/14 *Rocking Response of Equipment Anchored to a Base Foundation.* Nicos Makris and Cameron J. Black. September 2001.

PEER 2001/13 *Modeling Soil Liquefaction Hazards for Performance-Based Earthquake Engineering.* Steven L. Kramer and Ahmed-W. Elgamal. February 2001.

PEER 2001/12 *Development of Geotechnical Capabilities in OpenSees.* Boris Jeremić. September 2001.

PEER 2001/11 *Analytical and Experimental Study of Fiber-Reinforced Elastomeric Isolators*. James M. Kelly and Shakhzod M. Takhirov. September 2001.

PEER 2001/10 *Amplification Factors for Spectral Acceleration in Active Regions.* Jonathan P. Stewart, Andrew H. Liu, Yoojoong Choi, and Mehmet B. Baturay. December 2001.

PEER 2001/09 *Ground Motion Evaluation Procedures for Performance-Based Design*. Jonathan P. Stewart, Shyh-Jeng Chiou, Jonathan D. Bray, Robert W. Graves, Paul G. Somerville, and Norman A. Abrahamson. September 2001.

PEER 2001/08 *Experimental and Computational Evaluation of Reinforced Concrete Bridge Beam-Column Connections for Seismic Performance*. Clay J. Naito, Jack P. Moehle, and Khalid M. Mosalam. November 2001.

PEER 2001/07 *The Rocking Spectrum and the Shortcomings of Design Guidelines.* Nicos Makris and Dimitrios Konstantinidis. August 2001.

PEER 2001/06 *Development of an Electrical Substation Equipment Performance Database for Evaluation of Equipment Fragilities*. Thalia Agnanos. April 1999.

PEER 2001/05 *Stiffness Analysis of Fiber-Reinforced Elastomeric Isolators.* Hsiang-Chuan Tsai and James M. Kelly. May 2001.

PEER 2001/04 *Organizational and Societal Considerations for Performance-Based Earthquake Engineering.* Peter J. May. April 2001.

PEER 2001/03 *A Modal Pushover Analysis Procedure to Estimate Seismic Demands for Buildings: Theory and Preliminary Evaluation.* Anil K. Chopra and Rakesh K. Goel. January 2001.

PEER 2001/02 *Seismic Response Analysis of Highway Overcrossings Including Soil-Structure Interaction.* Jian Zhang and Nicos Makris. March 2001.

PEER 2001/01 *Experimental Study of Large Seismic Steel Beam-to-Column Connections.* Egor P. Popov and Shakhzod M. Takhirov. November 2000.

PEER 2000/10 *The Second U.S.-Japan Workshop on Performance-Based Earthquake Engineering Methodology for Reinforced Concrete Building Structures.* March 2000.

PEER 2000/09 *Structural Engineering Reconnaissance of the August 17, 1999 Earthquake: Kocaeli (Izmit), Turkey.* Halil Sezen, Kenneth J. Elwood, Andrew S. Whittaker, Khalid Mosalam, John J. Wallace, and John F. Stanton. December 2000.

PEER 2000/08 *Behavior of Reinforced Concrete Bridge Columns Having Varying Aspect Ratios and Varying Lengths of Confinement.* Anthony J. Calderone, Dawn E. Lehman, and Jack P. Moehle. January 2001.

PEER 2000/07 *Cover-Plate and Flange-Plate Reinforced Steel Moment-Resisting Connections.* Taejin Kim, Andrew S. Whittaker, Amir S. Gilani, Vitelmo V. Bertero, and Shakhzod M. Takhirov. September 2000.

PEER 2000/06 *Seismic Evaluation and Analysis of 230-kV Disconnect Switches.* Amir S. J. Gilani, Andrew S. Whittaker, Gregory L. Fenves, Chun-Hao Chen, Henry Ho, and Eric Fujisaki. July 2000.

PEER 2000/05 *Performance-Based Evaluation of Exterior Reinforced Concrete Building Joints for Seismic Excitation.* Chandra Clyde, Chris P. Pantelides, and Lawrence D. Reaveley. July 2000.

PEER 2000/04 *An Evaluation of Seismic Energy Demand: An Attenuation Approach.* Chung-Che Chou and Chia-Ming Uang. July 1999.

PEER 2000/03 *Framing Earthquake Retrofitting Decisions: The Case of Hillside Homes in Los Angeles.* Detlof von Winterfeldt, Nels Roselund, and Alicia Kitsuse. March 2000.

PEER 2000/02 *U.S.-Japan Workshop on the Effects of Near-Field Earthquake Shaking.* Andrew Whittaker, ed. July 2000.

PEER 2000/01 *Further Studies on Seismic Interaction in Interconnected Electrical Substation Equipment.* Armen Der Kiureghian, Kee-Jeung Hong, and Jerome L. Sackman. November 1999.

PEER 1999/14 *Seismic Evaluation and Retrofit of 230-kV Porcelain Transformer Bushings*. Amir S. Gilani, Andrew S. Whittaker, Gregory L. Fenves, and Eric Fujisaki. December 1999.

PEER 1999/13 *Building Vulnerability Studies: Modeling and Evaluation of Tilt-up and Steel Reinforced Concrete Buildings.* John W. Wallace, Jonathan P. Stewart, and Andrew S. Whittaker, editors. December 1999.

PEER 1999/12 *Rehabilitation of Nonductile RC Frame Building Using Encasement Plates and Energy-Dissipating Devices.* Mehrdad Sasani, Vitelmo V. Bertero, James C. Anderson. December 1999.

PEER 1999/11 *Performance Evaluation Database for Concrete Bridge Components and Systems under Simulated Seismic Loads.* Yael D. Hose and Frieder Seible. November 1999.

PEER 1999/10 *U.S.-Japan Workshop on Performance-Based Earthquake Engineering Methodology for Reinforced Concrete Building Structures.* December 1999.

PEER 1999/09 *Performance Improvement of Long Period Building Structures Subjected to Severe Pulse-Type Ground Motions*. James C. Anderson, Vitelmo V. Bertero, and Raul Bertero. October 1999.

PEER 1999/08 *Envelopes for Seismic Response Vectors.* Charles Menun and Armen Der Kiureghian. July 1999.

PEER 1999/07 *Documentation of Strengths and Weaknesses of Current Computer Analysis Methods for Seismic Performance of Reinforced Concrete Members.* William F. Cofer. November 1999.

PEER 1999/06 *Rocking Response and Overturning of Anchored Equipment under Seismic Excitations.* Nicos Makris and Jian Zhang. November 1999.

PEER 1999/05 *Seismic Evaluation of 550 kV Porcelain Transformer Bushings.* Amir S. Gilani, Andrew S. Whittaker, Gregory L. Fenves, and Eric Fujisaki. October 1999.

PEER 1999/04 *Adoption and Enforcement of Earthquake Risk-Reduction Measures.* Peter J. May, Raymond J. Burby, T. Jens Feeley, and Robert Wood.

PEER 1999/03 *Task 3 Characterization of Site Response General Site Categories*. Adrian Rodriguez-Marek, Jonathan D. Bray, and Norman Abrahamson. February 1999.

PEER 1999/02 *Capacity-Demand-Diagram Methods for Estimating Seismic Deformation of Inelastic Structures: SDF Systems*. Anil K. Chopra and Rakesh Goel. April 1999.

PEER 1999/01 *Interaction in Interconnected Electrical Substation Equipment Subjected to Earthquake Ground Motions.* Armen Der Kiureghian, Jerome L. Sackman, and Kee-Jeung Hong. February 1999.

PEER 1998/08 *Behavior and Failure Analysis of a Multiple-Frame Highway Bridge in the 1994 Northridge Earthquake.* Gregory L. Fenves and Michael Ellery. December 1998.

PEER 1998/07 *Empirical Evaluation of Inertial Soil-Structure Interaction Effects.* Jonathan P. Stewart, Raymond B. Seed, and Gregory L. Fenves. November 1998.

PEER 1998/06 *Effect of Damping Mechanisms on the Response of Seismic Isolated Structures.* Nicos Makris and Shih-Po Chang. November 1998.

PEER 1998/05 *Rocking Response and Overturning of Equipment under Horizontal Pulse-Type Motions.* Nicos Makris and Yiannis Roussos. October 1998.

PEER 1998/04 *Pacific Earthquake Engineering Research Invitational Workshop Proceedings, May 14–15, 1998: Defining the Links between Planning, Policy Analysis, Economics and Earthquake Engineering.* Mary Comerio and Peter Gordon. September 1998.

PEER 1998/03 *Repair/Upgrade Procedures for Welded Beam to Column Connections.* James C. Anderson and Xiaojing Duan. May 1998.

PEER 1998/02 *Seismic Evaluation of 196 kV Porcelain Transformer Bushings.* Amir S. Gilani, Juan W. Chavez, Gregory L. Fenves, and Andrew S. Whittaker. May 1998.

PEER 1998/01 *Seismic Performance of Well-Confined Concrete Bridge Columns.* Dawn E. Lehman and Jack P. Moehle. December 2000.